# Hydrocarbon Detection with Metal Oxide Semiconducting Gas Sensors Modified by Overlayer or Admixture of Zeolites Na-A, H-Y and H-ZSM-5

Authors: P. Tarttelin Hernández,[a] S. M. V. Hailes[b], and I. P. Parkin[c]*

Affiliations: [a] Dept. of Security and Crime Science, University College London, 35 Tavistock Sq., London, WC1H 9EZ, UK E-mail: paula.tarttelin.10@ucl.ac.uk
[b] Dept. of Computer Science, University College London, Gower St., London, WC1E 6BT, UK. E-mail: s.hailes@ucl.ac.uk
[c] *Dept. of Chemistry, University College London, 20 Gordon St, London, WC1H 0 AJ, UK. E-mail: i.p.parkin@ucl.ac.uk; Fax: +44 (0)20 7679 7463; Tel: +44 (0)20 7679 4669
Electronic supplementary information (ESI) available: See DOI: 10.1039/b000000x/

## Abstract

A control thick-film $SnO_2$ gas sensor was modified with zeolites holding LTA, FAU and MFI frameworks using two different approaches to integrate them into the gas-sensing interface. The objective was to prompt selectivity and sensitivity enhancements that were otherwise unattained with the unmodified material when detecting a range of hydrocarbon vapours with similar molecular structures and kinetic diameters. Molecules with different functional groups were also explored. Overlayers were designed by screen-printing 1 or 3 zeolite depositions on top of the control sensor. Admixtures were prepared by screen-printing composites of the control material with 10 % (w/w) and 30 % (w/w) of zeolite. Tests were performed against ethane, propane, butane, ethanol, isopropanol, acetone, toluene and carbon monoxide at concentrations in the 2.5-125 ppm range and sensors were heated to temperatures in the 250-500 °C range. Sensors were also exposed to humid air and to a mixture of ethane and humid air to assess the selective capabilities of the sensing materials in mixed-gas environments. Both fabrication methods provided sensor responses that, combined, favoured vapour discrimination in a way unachievable with the control sensor and the presence of zeolite was seen to assist in sensitivity and selectivity enhancements towards vapours, whilst providing stable and repeatable responses over time.

## 1.0 Introduction

Metal Oxide Semiconductors (MOS) are gas-sensitive resistors that show a reversible change in the conductivity of the sensing material when exposed to test gases at temperatures in the range of 150-600 °C.(1, 2) The versatility of MOS gas sensors makes them good candidates to detect vapours that pose a direct threat to air quality, climate change and health.(3-5) More recently, these sensors have also found a niche in the security field, enabling the monitoring of markers associated with explosive (6) or drug materials.(7, 8) The reason why markers are targeted for detection is because they have higher vapour pressures than the active ingredient itself, as in the case of explosive taggants and of solvents or additives used in drug manufacture. Several companies have commercialised MOS technology for hazardous gas detection and to monitor air quality, and the plausibility of e-noses to address security and military-related issues has been highlighted by a number of reports.(5, 9, 10)

The appeal of MOS sensors lies in their high sensitivity to part-per-million (ppm) and part-per-billion (ppb) levels of a wide range of vapours, the rapid response and recovery times that can be achieved, their low cost, small size and potential for portability.(1, 3, 11, 12) Nevertheless, the high power required for continuous operation and the sensors' inability to individually respond to vapours selectively constitute major drawbacks for mobile systems.(13-15) This may limit their usability to intermittent and/or localised detection environments where there is only one target vapour with little or no interference from competing vapours.(16) To circumvent this, it is possible to use a sensing array composed of a selected number of sensors, each responding to a vapour at a different rate and to a greater or lesser degree, producing a fingerprint that is unique for each gas.

Recent research efforts have been principally aimed at improving the discriminating capabilities of either individual sensors or sensing arrays when exposed to mixed-gas environments.(14, 17-20) It has been shown that sensitivity and selectivity enhancements are frequently seen upon modification of the surface microstructure of the control sensing material by addition of catalytically active agents and/or porous materials with high surface area, the framework structure of which is strategically used to induce molecular filtering. Given that MOS sensors typically see a sensitivity maximum when they are heated over a specific temperature range and this maximum will change with gas type, temperature modulation serves as an additional means of achieving selectivity.(21, 22)

Zeolites are crystalline aluminosilicates that consist of tetrahedral $SiO_4$ and $AlO_4$ linked through oxygen atoms to form 3D frameworks with pores of molecular size.(23) Their role as catalytic filters has been increasingly used in recent years and their physicochemical properties make them perfectly suited to prompt selectivity and sensitivity enhancements in gas sensors. The zeolite framework has a net negative charge compensated by introduction of cations that are able to move through the cavities of the zeolites, assisting in catalytic reactions and leading to rich ion-exchange chemistry.(24)

The framework and composition of zeolites will directly affect their chemical properties such that high aluminium content (low Si/Al ratio) will result in a hydrophilic character as seen, for instance, in zeolites with an LTA framework. Conversely, low aluminium content (high Si/Al ratio) will lead to a hydrophobic character as seen, for instance, in zeolites with an MFI framework.(22) The Si/Al ratio determines the acidic centres per unit cell and content of mobile cations, which consequently affects the ionic conductivity of the material when interacting with gas molecules.(24) Furthermore, their internal porosity leads to high surface areas with surface-reactive sites that favour strong interactions between the pore walls of zeolites and gas molecules. Zeolite incorporation in gas sensors has been seen to assist in separating and detecting trace concentrations of vapours.(14, 22) In combination with n- and p-type materials, zeolites are particularly efficient at selectively targeting saturated and unsaturated hydrocarbon vapours, solvents and inorganic gases like $NO_2$.(6, 17, 18, 24-27)

The incorporation of zeolite materials into MOS gas-sensing systems has mostly been in the form of layers on top of the control material, referred to as overlayers or coatings.(16, 22, 25, 28-30) Used as a physical barrier between the metal semiconductor and the air/gas atmosphere, they assist in filtering molecules according to shape/size.(14, 20, 31) The thickness of the zeolite film influences sensor selectivity, sensitivity and response times such that the thicker the zeolite overlayer, the better the selectivity and the slower the response times.(32) Although MOS admixtures (powders mixed with zeolites in organic ink), have received less attention in the literature, recent studies carried out by our group have shown outstanding improvements in the sensing properties of the sensors.(6, 8, 27, 33)

In this study, a control $SnO_2$ material was modified by zeolite incorporation with the aim of inducing microstructural changes that could improve the overall performance of the sensors. To the best of our knowledge it is the first time that a control screen-printed $SnO_2$ sensor has been modified by additional screen-printed overlayers of zeolites H-ZSM-5, H-Y and Na-A and by admixture with the zeolites. These zeolites were chosen to explore the effects of crystal topology, size and morphology on the performance of the sensors when exposed to a range of reducing gases with similar molecular structure and kinetic diameters. The sensing arrays have been tested in the presence of trace vapour concentrations of alkanes of different length (ethane, propane, butane) and of molecules with different functional groups (ethanol, isopropanol, acetone, carbon monoxide and toluene). Sensors were exposed to different concentrations of gases and heated to temperatures ranging from 250 °C to 500 °C. Sensor sensitivity to water vapour was also evaluated and, in order to test the selective capabilities of the arrays, they were later exposed to a mixture of ethane and humid air at different relative humidities (RH).

The sensing arrays devised here proved very successful in discriminating among hydrocarbon vapours, regardless of similarities in molecular structure, kinetic diameter or functional group and this was possible across the full range of temperatures tested. Stable and repeatable results were obtained, particularly at higher temperatures. With zeolite incorporation, trace detection of vapours was remarkably improved and, although some sensors were able to individually respond to a vapour more sensitively and suppress the response to another, they were most effective when used in combination with other sensors.

## 2.0 Methodology

### 2.1 Sensor Assembly & Experimental Gas-sensing Procedure

$SnO_2$ is one of the most widely used materials in gas sensing due to its excellent sensitivity and stability in reducing atmospheres and due to its low cost.(34) Material inks were made by mixing commercial $SnO_2$ powder (Sigma Aldrich) with an organic vehicle (ESL 400). Zeolite powders H-ZSM-5 and H-Y were obtained from Zeolyst International, USA (H-ZSM-5 CBV 8014 and Y-zeolite CBV 600) and zeolite Na-A from Advera PQ-Corporation. Zeolites H-Y and H-ZSM-5 were employed in the hydrogen form and the sodium cation was used in zeolite A. Zeolite powders were also mixed with the ESL 400 organic vehicle to produce printable inks. Metal oxide inks were prepared and treated as in (8). An illustration of the types of sensors that were prepared is presented in Fig. 1.

Zeolite H-ZSM-5 has an MFI framework with Si/Al = 140 and 10 rings with pore dimensions 5.1 x 5.5 and 5.3 x 5.6 (Å). Zeolite H-Y holds a FAU framework, with Si/Al ratio = 2.55 and 12 rings with pore dimensions 7.4 x 7.4 (Å). Zeolite Na-A has a LTA framework with Si/Al = 1.2 and has 8 rings with pore apertures of 4.1 x 4.1 (Å). The control sensor was fabricated by screen-printing five layers of $SnO_2$ on the surface of a 3 x 3 mm alumina substrate that has interdigitated gold electrodes on the obverse of the sensor chip and has an integrated heater track underneath to enable its heating. Zeolite overlayers were prepared by mixing zeolite powders with the organic vehicle and then screen-printing the material on top of the control $SnO_2$ layers (Fig.1). The effect of increasing the number of zeolite coatings was investigated by printing either one or three additional film depositions on top of the control material. Zeolite admixtures were prepared by mixing the metal oxide and zeolite powders

together with the organic vehicle. The control was mixed with 10 % (w/w) or 30 % (w/w) of zeolites H-ZSM-5, H-Y and Na-A. The number of layers of the control material was five. Sensors were sintered at 600 °C for an hour. Aside from the control $SnO_2$ sensor, referred to as CTL in graphs, there were two sets of sensing arrays, the details of which have been presented in Table 1.

Test vapours were introduced into a stream of dry baseline air ($R_0$) in five 10-minute pulses. The source cylinder concentration was diluted in a stream of synthetic air to investigate a range of concentrations as follows: 5 %, 10 %, 25 %, 50 %, 80 % and 100% of the total cylinder concentration, which has been specified in brackets for each gas below. This allowed the sensor resistance in the presence of target gas to be determined. Gases were obtained from and certified by BOC gases: isopropyl alcohol (500 ppm), ethanol (100 ppm), acetone (10 ppm), toluene (50 ppm), ethane (100 ppm), propane (100 ppm) and butane (100 ppm), carbon monoxide (1000 ppm). Trace vapour concentrations were evaluated with the aim of assessing the relevance of the arrays in real life applications, which often require vapour detection at the ppm and ppb levels, such as in the case of Volatile Organic Compound (VOC) monitoring for air quality purposes, as alarm and security systems and for medical diagnostics. Experiments were carried out at temperatures between 250 °C and 500 °C. In order to assess whether the sensors provided repeatable responses each test was repeated at least three times. When possible, tests were also repeated at a later date to ensure sensor stability. Because the sensors were used on and off for a period of approximately 4-5 months, it was important to check if over time the sensing results were consistent with previous data.

### 2.2 Material Characterisation

Sensor characterisation was performed on all sensing materials to better understand how the vapours may interact with the different surface microstructures. X-Ray diffraction (XRD) was carried out on a Bruker D8 discover diffractometer with Cu Kα1/Kα2 radiation (λ = 1.5418 Å) X-ray source operating at 30 W with a Vantec 500 detector. XRD patterns were collected over the 2θ range 15 - 70°, with a time step of 100 s/step x 3 steps, using a 1 mm collimator.

Scanning Electron Microscopy (SEM) was carried out on a Phillips XL30 environmental scanning electron microscope. The micrographs displayed below were collected at a magnification of x10000, although additional magnifications were investigated. The film thickness of the sensors was assessed with a Hitachi S-3400N microscope operated at 5 kV using a working distance of approximately 16 mm.

## 3.0 Results & Discussion

### 3.1 Sensor Characterisation

$SnO_2$ powders were mixed with an organic vehicle, making it into ink suitable for screen-printing onto 3 × 3 mm alumina substrates. The $SnO_2$ sensing material was modified by incorporation of zeolites in the form of admixtures or overlayers on top of the control as illustrated in Fig. 1. The inks were fired in a furnace at 600 °C for one hour in order to sinter the material and to evaporate the organic vehicle. Physicochemical characterisation techniques revealed that the fabrication process and heat exposure did not affect the crystalline structure of the materials.

**3.1.1 X-Ray Diffraction.** The materials kept their crystalline structure despite heat exposure during the fabrication process. The XRD pattern of the control $SnO_2$ material could be identified in all samples, regardless of the fabrication method. The XRD pattern of $SnO_2$ was tetragonal in structure with characteristic 2θ peaks at 26.5 (110), 33.8 (101), 38.1 (200), 38.9 (111), 51.7 (211), 54.7 (220), 57.7 (002) and 61.8 (310). As expected, the peaks corresponding to the zeolites were more intense in the sensors fabricated with overlayers than in the admixed ones. This has been illustrated in Figure 2.

### 3.1.2 Scanning Electron Microscope.

The particles in the control $SnO_2$ sensor were round in shape and interconnected. Micrographs of the sensor chip at x20 magnification (not shown) revealed a pattern on the outermost layer of the sensing material that was left by the screen-printing mesh whilst spreading the ink, which was modestly uniform, showing clear craters and ridges throughout. The particles were ~100 - 200 nm in size.

*Admixtures:* The presence of the control material was clear in all the sensors that were fabricated by mixing with zeolites (Fig.3). The progressive increase in zeolite loading was also evident in the SEM images. The zeolite materials were poorly visible in admixtures containing 10 % (wt.) of zeolite. These sensors exhibited an external layer with an appearance resembling that of the control sensing material. Although the porosity of the materials was still evident, the surface of the admixtures appeared to be denser than that of the overlayers.

*Overlayers:* The particles of the overlaid H-Y sensors showed sharper edges and appeared to be ~500 nm in size (not shown). The surface of this material was also porous with visible cavities. The surface of the sensor containing three layers of zeolite H-Y was slightly different to that containing one layer; the shape of the particles was less well defined and appeared flatter. This could be the result of more pressure inflicted by the mesh as more layers were being deposited onto the chips. The material in the latter case was mechanically unstable and would easily detach from the chip when handled. This could be due to poor sintering. The sensors containing layers of zeolite Na-A showed particles cubic in shape with round edges that differed in size. Whilst most particles appeared to have an average size of ~2 µm, some of them were as small as ~400 nm. The overlayers containing zeolite H-ZSM-5 had particles with considerably different sizes and were smooth around the edges. As in the case of the other zeolites, there were cavities present in the structure. The film thickness corresponding to 5 layers of the control $SnO_2$ material was ~ 130 µm and the layer of zeolite H-ZSM-5, which was used for guidance corresponded to ~26 µm (Fig. 4).

## 3.2 Gas Sensing Results

Exposure of an n-type material to a reducing gas will typically result in a decrease in the resistance of the sensing material. At high temperatures the resistance of metal semiconductors changes when exposed to vapours that are able to react with oxygen species chemisorbed at the surface of the sensing material.(36) In the presence of slightly humid air and at temperatures in the 150 – 450 °C, these oxygen species exist mostly in the form of $O^-$, which act by trapping electrons at the surface.(13) Reducing gases like ethanol will react and remove oxygen species adsorbed at the surface, releasing the previously trapped oxygen electrons back into the oxide. This results in the specified decrease in resistance. The sensor response is thus calculated as the ratio of the sensor's resistance in air ($R_0$) to that in the presence of gas (R), termed conductive response. In the case where the resistance of an n-type material increased upon exposure to a gas, the response was calculated as $R/R_0$ and termed resistive response.

In this study zeolites with contrasting Si/Al ratios and pore sizes (H-ZSM-5, H-Y and Na-A) were incorporated to the control sensing material using two different approaches; (1) one or three overlayers were used as filtering elements and (2) the $SnO_2$ material was mixed with different zeolite loadings for comparison purposes. The arrays were tested in the presence of trace vapour concentrations of alkane chains of different length (ethane, propane, butane) and of molecules with different functional groups (ethanol, isopropanol, acetone, toluene and carbon monoxide). A test was also performed against an oxidising gas ($NO_2$) to ensure the materials behaved by showing a decrease in conductivity (not shown).

The detection temperature and the supplied gas concentrations were gradually modified to determine the temperature at which the sensor's sensitivity to a gas was highest and whether the sensors responded linearly to progressively increased concentrations of vapour, whilst providing repeatable and stable results over time. Tests were also performed in humid conditions and also by

mixing ethane with humid air at 10 % and 25 % RH to further explore the selective potential of the sensors.

Note that the response time is the time taken by the sensor to reach 90% of the maximum resistance value, termed $t_{90}$. The recovery time is the time taken by the sensor to return to within 10% of its initial baseline value when the test gas is switched off.

### 3.2.1 Concentration and Temperature Effects.

The control $SnO_2$ sensing material was initially exposed to six different concentrations of ethanol vapour (5 – 100 ppm) and was heated across a range of five temperatures (250 - 500 °C) shown in Fig. 5. The sensor behaved as expected, showing an increase in conductivity when exposed to the gas.

Raising the concentration of gas supplied resulted in an increase in sensor response $R_0/R$. The sensor's optimal temperature was 300 °C with $R_0/R_{(100ppm\ EtOH)}$ ~ 12 (SD ±0.4). It was found that the responsivity of the sensor could vary more markedly at lower temperatures when performing repeat tests at concentrations exceeding 50 ppm. For instance, at 250 °C $R_0/R_{(100ppm\ EtOH)}$ was ~10 (SD ± 1.6), providing a 15 % difference in sensor responses from three repeats. Large error margins have long been reported as an issue associated with $SnO_2$ gas-sensing materials.(37-39)

The control sensor was then supplied with IPA concentrations ranging between 25 and 125 ppm and at temperatures in the range of 300 °C - 450 °C. Similarly, at 300°C there was more variability in the sensor responses $R_0/R$ = 12.34 (SD ± 1.0), when compared to higher temperatures like 450 °C $R_0/R$ = 5.26 (SD ± 0.1). The unmodified $SnO_2$ sensor was unable to differentiate between ethanol and IPA vapours across the full temperature range (Fig. 5).

Given the higher error margins seen at lower temperatures, tests on other gases were performed at 350 °C, 400 °C and 450 °C. It was revealed that in general at 450 °C the response and recovery times were improved and the sensing element would saturate more quickly, attaining steady state easily. The control sensor failed to produce markedly different responses when exposed to acetone (10 ppm) and butane (100 ppm) at this temperature and it was also the case for ethane and propane vapours across the full temperature range. Exposure to ethane and propane lead to a mild increase in response when raising concentration and temperatures.

The optimal temperature of the zeolite-modified sensors did not always match the optimal temperature of the control. Although incremental zeolite depositions (3 layers) affected sensor sensitivity to gases when compared to sensors containing only 1 layer, the temperature at which sensitivity to a particular gas was highest remained the same for each zeolite group. This was not true for the admixtures. The zeolite loading in the admixtures directly affected the optimal temperature of the sensors when they were exposed to different gases. This behaviour has also been found in other studies based on admixtures with n-type (6, 27) and p-type materials (33). Therefore, the way in which the sensing material was combined with the zeolites often resulted in contrasting effects on sensitivity and selectivity to vapours.

### 3.2.2 Microstructural Effects: Introducing Zeolites to the Control Sensing Element

The response of a sensor to a gas may be affected by the *diffusion* of a vapour through the sensing material, the *rate of the reaction processes* and the *type of reactions or interactions* occurring at the surface of the sensor.(14,22) This section evaluates how the introduction of zeolites to the sensing element in the form of admixtures and overlayers influenced sensor responses; diffusion, kinetic and reaction factors have been discussed. The effects of zeolite incorporation on gas discrimination have also been discussed.

As described by Binions et al (2011) the sensor microstructure plays a key role in the kinetics of reactions taking place at the sensor surface; a more porous microstructure introduces a high area-to-volume ratio to the sensing element, consequently amplifying the concentration of surface-reactive

sites that assist in the promotion of the overall conductivity of the sensing system. In the presence of a target vapour the sensing material may react with it such that an enhancement or diminution of the sensor response may be observed. This is a direct result of the sensitivity of the sensing element to the reactions products. That is, where the sensing element is highly sensitive to the reaction product(s) its response will increase. In the case where the sensor is less sensitive to the reaction product(s), its response will decrease.

Several studies have investigated the effects of incorporating zeolites as additional coatings over the sensing material as a means to promote an enhancement in the response of conventional oxide sensors and to favour the exclusion of interfering molecules. The structural features of zeolites can serve to fine-tune the passage of gas molecules through the zeolite layers according to the shape and/or size of the target molecules. Nevertheless, they may introduce a delay in the response time of the sensor due to an added resistance imposed by the coating, depending on the structural framework and pore dimensions of the zeolite and its particular interaction with the target gas. This increase in response time occurs because the zeolite layers hinder the direct interaction between the gas molecules and the underlying sensing material affecting gas diffusion. Gas molecules that are similar in size or larger than the zeolite pores may still diffuse through the cracks or voids in the system, however, this the diffusion rate will be slow enough that diffusion can be deemed negligible. The effects of delays in response times on oxide-zeolite mixtures have not been discussed in the literature. Although the lagged response can also be expected due to the zeolite presence, it may be less apparent due to the direct access of the gas molecules to the sensitive material.

As alluded to previously, the catalytic properties of zeolites may lead to reaction products different to those obtained with the unmodified material. Zeolites are used as cracking agents that can break the source gas molecules into other products. (14) This can thus result in an increase or decrease of the sensor response according to the sensitivity of the sensor to such reaction products.

As described in section 3.2.1 the unmodified sensor was unable to differentiate between some of the molecules that were tested. As an example, it would be expected that gases with similar molecular structures and functional groups, such as EtOH and IPA, would react similarly with the sensor surface. As shown in Fig. 5, the magnitude of the response of the control towards both gases was identical and the peak shapes (not shown) were as well. For this reason, the surface microstructure of the control $SnO_2$ material was altered in different ways: using zeolites as cover layers or as admixtures.

By looking at different detection temperatures and different fabrication procedures it was possible to distinguish between gases that were previously unresolved with the control sensing material. The section presented below focuses on sensor responses to acetone, toluene, ethanol and isopropanol vapours at 450 °C, given that the overall performance of the sensors at this temperature was improved.

Overlayers were used as a physical barrier between the metal semiconductor and the air/gas atmosphere as they assist in filtering molecules according to shape/size. This means that molecules with small kinetic diameters can diffuse through cracks or voids in the material or through pores in zeolites that are big enough to enable their diffusion to the underlying sensing material, whilst larger molecules may be filtered out. In the case of the admixtures, it is possible that the enhancements in sensitivity are due to the direct access of the vapours to the control sensing material (refer to the SEM images in Figure 3). The smaller particle size of the control and the presence of zeolite could lead to more surface-reactive sites for the gases to interact than when confronted with just the zeolite coatings.

The presence of acidic centres in the zeolite framework may accelerate reactions and also lead to reaction products different to those obtained with the unmodified sensor, the responsiveness of which will be directly influenced by the inherent sensitivity of the underlying sensing material to the gas and/or its reaction products.(14) Alternatively, diffusion of the gas into the sensitive layer may be

slowed down due to percolation effects brought about by the zeolite, characterised by response shapes that resemble a shark fin. This is discussed further below.

#### 3.2.2.1 Inspection of Peak Shapes, Response and Recovery Times.

Inspecting the peak shapes when exposing the sensors to hydrocarbon vapours revealed that at high temperatures such as 450 °C fast responses occurred, characterised by flat peak shapes, consistent with reaching steady state. These fast responses seen with hydrocarbon exposure at 450 °C could potentially be the result of complete combustion reactions leading to the production of $CO_2$ and water vapour. It may therefore be the case that in the elevated temperature range the reactions are essentially surface-driven. As the temperature was progressively lowered, vapour discrimination was more effective, often resulting in large enhancements in sensitivity. Diffusion through the voids and cracks in the sensing material leads to slower response times, characterised by shark-fin peak shapes; the vapour is able to react inside the zeolite pores and it could potentially produce different reaction products that have higher affinity towards the sensing material than the original supplied vapour. This could explain the notable differences in sensitivity when testing across different temperatures.

In the lower temperature range (i.e. 300 °C or 350 °C) it was often the case that when a sensor was particularly sensitive to a vapour it became more difficult to attain repeatable responses. This could be due to the vapour being effectively trapped in the material and zeolite pores, consequently being poorly desorbed. This behaviour was particularly evident with sensors modified with zeolite overlayers and this was most common with Na-A zeolite. As discussed beforehand, this zeolite is hydrophilic in nature and $SnO_2$ has also been reported to show an affinity for water.(20) It is therefore possible that water molecules produced as part of the reaction processes would act as competing substances and would be retained in the zeolite pores. The thick physical barrier of the zeolite could also be more effective at retaining moisture and not desorbing it efficiently following gas pulses, preventing the sensor's resistance from returning to baseline. At higher temperatures the size of the zeolite pores may distend (40), permitting the diffusion of molecules that would otherwise be more effectively hindered from diffusing at lower temperatures. The high sensitivity of zeolite H-ZSM-5 in both overlayers and admixtures when exposed to toluene in the higher temperature range may be an example of this. Sensitivity towards toluene was highest at 400 °C and, given that the pores of H-ZSM-5 are too small for the straightforward diffusion of this molecule, it is possible that at higher temperatures the molecules become less rigid and the zeolite pores slightly larger than reported as part of crystallographic calculations.(40) It must be noted that in this case, however, the enhanced sensitivity obtained with this zeolite might be the result of affinity between the hydrophobic nature of the zeolite and the lower polar character of toluene.

Figure 7 shows the relationship between the types of zeolite used in this study and their interaction with ethanol, IPA, toluene and acetone vapours. The response time ($t_{90}$) for each sensor has also been included. It can be seen that more zeolite layers of Na-A delayed the response to the vapours tested. Although the incorporation of one layer of zeolite Na-A improved the response to ethanol and IPA only slightly, the response was considerably improved (by a factor of 4) when incorporating 3 layers. The smaller kinetic diameter of ethanol favours its diffusion into the sensing material, whereas the branched IPA molecule may experience more difficulty in passing through. Sensor responses to IPA were very similar, regardless of the number of zeolite Na-A layers. The modest enhancement in sensitivity when compared to the control could be attributed to the hydrophilic character of the zeolite and the polarity of the IPA molecule.

The response towards acetone was worsened with the addition of Na-A overlayers. Despite the similar kinetic diameters of IPA, ethanol and acetone, the underlying sensing material was not particularly sensitive to acetone. Nevertheless, it must be noted that the concentration of acetone was much lower (8ppm) than that of ethanol and IPA. Given that the polarity of ethanol and IPA is higher than that of acetone, it may also contribute to lower sensitivity of this sensor to the vapour.

At 450 °C sensors were generally more sensitive to the vapours when they were covered with 3 film depositions of zeolite. Regarding the admixed sensors, 10 % (w/w) Na-A resulted in a remarkable increase in sensitivity to ethanol, IPA and acetone, when compared to 30 % (w/w) Na-A and the control sensor. Although the improvement in sensitivity was more conservative, sensors admixed with 30 % (w/w) H-Y also showed an enhancement in response when exposed to the four gases. However, '10 % (w/w) H-Y' was slightly more sensitive to ethane, propane and butane than its counterpart. Sensors admixed with zeolite H-ZSM-5 responded similarly when exposed to toluene and acetone, irrespective of the amount of zeolite loading. It is noteworthy that although it did so discreetly, the 10 % (w/w) H-ZSM-5 improved the responses to straight-chain alkanes.

### 3.2.2.3 Effects of Zeolite Incorporation on Sensitivity & Selectivity

It was revealed that sensors did not always follow the behaviour of an n-type material and this behaviour occurred specifically with alkane exposure and it varied with temperature. The control sensing material behaved as a p-type semiconductor when exposed to ethane and propane at 350 °C and 400 °C and this behaviour was stimulated further by the presence of zeolites (Fig. 8). As an example, whilst sensors overlaid with zeolites H-Y and H-ZSM-5 showed an increase in conductivity when exposed to ethane at 450 °C, sensors overlaid with zeolite Na-A appeared to be unresponsive to the gas. As the temperature was gradually dropped to 350 °C all zeolite-overlaid sensors (H-ZSM-5, H-Y and Na-A) showed responses consistent with p-type behaviour when supplied with ethane vapour. Sensors fabricated as admixtures behaved differently, often providing great enhancements in sensitivity. At 450 °C only certain sensors showed an increase in resistance with alkane exposure but at temperatures between 300 °C and 400 °C, all sensors consistently showed an increase in resistance. This could be due to the production of new reaction products, see section 3.2.2.1 below.

To illustrate the great differences in sensitivity obtained across fabrication methods, at 400 °C the resistive response to 100 ppm ethane seen with '10 % (w/w) LTA' was $R/R_0$ ~9 (SD ± 0.5), compared to $R/R_0$ ~1.3 (SD ± 0.01) and ~1.4 (SD ± 0.02) obtained with the sensors overlaid with 1 and 3 layers of zeolite Na-A, respectively. At 350 °C the response $R/R_0$ to 100 ppm ethane with '10% (w/w) Na-A' was ~12 (SD ± 0.3), yet sensors coated with Na-A were virtually unresponsive to it.

With the exception of toluene exposure, which lead to poor sensor recovery in some sensors, it was generally the case that sensor performance was fit for purpose; sensitive to trace vapour concentrations and providing prominent response and peak shape differences when exposed to different vapours, providing very fast response and recovery times and reaching steady state. This makes them particularly strong candidates for selective MOS technology systems. Zeolite incorporation lead to great sensitivity enhancements and allowed discrimination between previously unresolved sensor responses to vapours of similar molecular structure. The sensors provided repeatable and stable responses over time, particularly at higher temperatures i.e. 400 °C and 450 °C.

*Sensor Exposure to Alkanes.* Given that p-type behaviour was affected by fabrication procedure and temperature, the following conclusions have been reached. It is possible that the observed p-type behaviour is due to the production of an oxidising gas such as acetic acid, formed as part of the reaction processes taking place at the sensor surface. Yin et al (2014) exposed $Ag/Ag_2SnO_3$ nanoparticles to ethanol and acetic acid, reporting an increase in resistance upon exposure to the gas, which may act as oxidising (41). This could indeed support the results found in this study i.e. the production of acetic acid due to the interaction of ethane with oxygen at the sensor surface. P-type behaviour in overlaid sensors was less common but it was observed occasionally in some sensors when heated to 350 °C, whereas some admixed sensors would begin to behave as p-type at 450 °C and by the time the temperature had been dropped to 350 °C they would all consistently behave as p-type.

The kinetic diameters of propane and butane are reported as 4.3 Å in the literature (42) and it is interesting to see how, despite the similarity in size, their interaction with the overlaid sensors

differed as a result of their shape; at 450 °C all sensors were more sensitive to butane than they were to propane and, although sensors coated with Na-A were slightly more sensitive to butane, they were virtually unresponsive to propane.

The higher sensitivity seen in the more hydrophobic sensors (H-ZSM-5 and H-Y) to butane could be attributable to its inferior polarity when compared to propane. The poor sensitivity seen in sensors containing zeolite Na-A can be explained by the hydrophilic character of the zeolite and the hydrophobic nature of the alkane chains. Furthermore, both butane and propane are too large to diffuse through the 4.1 Å sized pores of zeolite Na-A, which may be another contributing factor to poor sensitivity at this temperature. Exposure to ethane with overlaid sensors showed responses very similar to propane at 450 °C, and in the same order of magnitude. Although its kinetic diameter would enable its movement through the pores of Na-A, the poor sensitivity is attributable to its organic nature and poor affinity for a hydrophilic zeolite. When sensors were heated to 450 °C and overlaid with zeolites, responsivity would increase with chain length.

The admixed sensors behaved very similarly when they were exposed to butane and propane at 450 °C and they only behaved considerably differently at 350 °C. It is thought that the higher prevalence of p-type behaviour seen in the admixtures is due to the microstructure of the sensors, which enabled more direct access of the test vapours to $SnO_2$. It is possible that this microstructure favours the cracking of hydrocarbons to more polar and oxidising compounds with functional groups containing a carboxylic acid, the affinity of which is much greater towards zeolite Na-A, leading to much-increased responsivity towards the vapours. Note that, at 350 °C, sensors had the same order of response seen upon exposure to ethane and butane (10 % Na-A > 30 % HY > 30 % Na-A > 10 % H-ZSM-5 > 30 % H-ZSM-5), with quasi-identical peak shapes, though showing higher responsivity to ethane than to butane (Fig. 8). This could suggest that these hydrocarbons break down to similar reaction products on these sensing materials. Generally, the microstructure of the admixtures proved more successful in enhancing responses at lower temperatures and particularly when exposing the sensors to ethane and butane.

Other studies that investigated n-type materials like $SnO_2$ as gas sensors for hydrocarbon detection used coatings of zeolites with MFI and LTA structures. Vilaseca et al (2008) used a Pd- $SnO_2$ sensor coated with LTA layers and, albeit heating the sensors across 250 – 400 °C and exposing them to propane vapour, they did not find the increase in resistance reported here. In a different study, Vilaseca et al (2007) exposed the Pd- $SnO_2$ sensors with coatings of zeolites MFI and LTA to a range of vapours and across different temperatures and, once again, their sensors followed the expected n-type behaviour when exposed to reducing gases. This could be a direct effect of the palladium dopant, the microstructure of the sensors fabricated as zeolite films grown on top of the $SnO_2$ material or the much higher concentrations of gases they investigated.

*Sensor Exposure to Alcohols.* The responses to ethanol and IPA vapours that were previously unresolved with the control sensor were successfully separated with zeolite-containing sensors. With the exception of sensor '1 layer Na-A', which could not discriminate between 100 ppm of both alcohols at 450 °C, the remaining sensors produced response differences when compared to the control, also showing selectivity towards either gas, (Fig. 6). More specifically, the sensors that revealed selectivity were '3 L Na-A' towards ethanol, suggesting that the branched conformation of IPA was most likely hindered from diffusion, and '3 L H-ZSM-5', '10% (w/w) Na-A', '30 % (w/w) H-Y' all towards IPA (Fig. 6 and 7), possibly due to the formation of reaction products to which $SnO_2$ is more sensitive.

The overlaid sensors were exceptionally responsive to ethanol, particularly at 300 °C with '1 layer Na-A' providing a response of $R_0/R$ = 90.4 (SD ± 4.5) and '1 layer H-ZSM-5' $R_0/R$ = 60.9 (SD ± 3.9) but, as alluded to previously, there were associated downsides to testing in the lower temperature range. At 450 °C the sensors showed very fast response and recovery times, reaching steady state in <18 seconds with sensors '1 and 3 layers of Na-A' and '3 layers H-ZSM-5'. In the case of overlayer

exposure to ethanol, $t_{90}$ was always below 50 seconds, with '10% (w/w) Na-A' saturating in ~2 seconds. Although $t_{90}$ was generally lower upon exposure to ethanol rather than IPA, this trend was reversed in the admixtures (Fig.7).

At 450 °C the sensor that was most responsive to ethanol was that overlaid with '3 layers Na-A' with $R_0/R$ ~24 (Fig. 9). Although the kinetic diameter of ethanol is larger than the pores of zeolite Na-A, this affinity is due to the hydrophilic character of the zeolite. It can be seen how big an effect the functional group has on responsivity in hydrophilic-like sensors and how it can prove useful to use this strategically to target certain vapours (compare, for instance, to ethane responsivity). Despite ethanol's ability to travel through the pores of H-ZSM-5 it can be seen that, when overlaid, the response of H-ZSM-5 sensors towards this polar molecule was limited and remained very similar to that seen in the control.

Responsivity to ethanol decreased when compared to the control with H-Y overlayers and it remained very similar to the control when incorporated as admixtures. At 450 °C the number of layers in sensors containing H-ZSM-5 and H-Y made little difference to the sensor responses. The most pronounced difference in sensor response among zeolite groups was that produced by 3 layers of zeolite Na-A, when compared to 1 layer zeolite Na-A. The number of zeolite layers directly influenced response and recovery times and they did not always slow down the response and recovery times with increasing thickness of the zeolite layer (Fig. 7). For instance, 3 layers of zeolite H-ZSM-5 gave a very fast response, with steady state achieved, whereas the 1-layered sensor responded in a slow fashion. This feature could be used as a discriminatory element when using data mining tools like Support Vector Machines (SVM) to classify gases. Zeolite incorporation resulted in distinct differences when compared to the control. At temperatures in the range of 250 - 350 °C '3 layers of Na-A' would not return to baseline when ethanol was removed from the sensing atmosphere.

At 450 °C the overlaid sensor that was most responsive to 100 ppm IPA was that containing three layers of zeolite H-ZSM-5, providing a response $R_0/R$ ~9, compared to $R_0/R$ ~5 attained when exposed to ethanol. The responsivity of sensors coated with H-Y was lower than that of the control, as with ethanol exposure, but differences between both vapours were still evident. Sensors containing 10% (w/w) of zeolite Na-A and H-ZSM-5 were more responsive than the ones containing 30 % (w/w). Generally, the admixed sensors were more responsive to IPA than the overlayers.
The sensors were remarkably responsive to IPA at lower temperatures like 300 °C. As an example, sensor '1 layer Na-A' provided $R_0/R$ ~ 10 (SD ± 0.5) to 25 ppm and ~87 (SD ± 4.8) to 125 ppm. Responses obtained with '1 layer H-Y' and '1 layer H-ZSM-5' were comparatively lower - 12.9 SD ± 0.7 and 16 SD ± 3.3, respectively - but nevertheless significant.

*Sensor Exposure to Acetone.* Overlaid sensor exposure to acetone resulted in responsivity lower than that attained with the control at 400 °C and 450 °C and sensitivity was almost unaffected by increased concentrations of gas at these temperatures (Fig. 9). At 350 °C the '3 layered Na-A' sensor responded to 10 ppm acetone with $R_0/R$ ~5, a 2.4-fold increase over the control material. Nevertheless, this sensor's response was slow and did not reach steady state. Although the kinetic diameter of acetone (4.6 Å) is smaller than the pore diameters of zeolites H-ZSM-5 and H-Y, they were moderately responsive to the gas with responses $R_0/R < 3$.

When exposing the admixed sensors to acetone, responsivity was enhanced considerably in relation to the overlayers and the control sensor. It is thought that at 450 °C the high responsivity ($R_0/R$ ~8) seen in the 10 % (w/w) Na-A sensor was due to water formation as part of a surface reaction process and subsequent adsorption into the sensing material. This was supported by the peak shapes, which were distinct and specifically seen when testing against humid air (see section 3.2.2.5 below). Once again, the microstructure seen in the admixed materials could act in favour of acetone's combustion, leading to reaction products (i.e. $CO_2$ and $H_2O$) to which the sensors are more or less sensitive. This was supported by the peak shapes, which indicated fast reactions, quickly reaching

steady state. As the temperature was lowered to 350 °C, the peak shapes and sensitivity changed notably. It was revealed that at lower temperatures the sensitivity of the control sensor to humid air was suppressed (see section 3.2.2.5 below), which could mean that the interference with water formation as part of the combustion process was no longer influencing the sensing responses, favouring the free interaction of the gas with the more hydrophobic zeolites like H-Y, providing responses of $R_0/R$ >5 to 8 ppm of acetone vapour. It has been reported in the literature that the affinity of H-Y towards acetone is due to its ability to sit inside the super-cages of the zeolite.(26)

Note that, at some temperatures, certain sensors overlaid with the same zeolite could respond very similarly to a gas irrespective of the number of zeolite overlayers on top of the $SnO_2$ material. An example of this are the 1 and 3 layered sensors coated with zeolite H-ZSM-5 when exposed to acetone at 400 °C and 450 °C, which also worsened the response attained with the control sensor. This similarity in response output seen among sensors containing the same zeolite was common when the incorporation of zeolite worsened the response to a gas relative to the control and resulted in little or no sensitivity to a vapour. At 450 °C it was often the case that the responses corresponding to sensors containing layers of the same zeolite would be grouped together, i.e. H-ZSM-5 overlayers produced a markedly different response to those covered with H-Y and those were, in turn, different to Na-A-modified sensors. Despite this, differences in sensitivity attributed to the number of zeolite layers could typically be observed.

*Sensor Exposure to Toluene.* Sensors that contained H-ZSM-5 zeolite were particularly sensitive to toluene regardless of the fabrication method. Given that the large kinetic diameter of this molecule would affect its diffusion through the zeolite pores, it is likely that sensor sensitivity is a consequence of hydrophobic affinity between the zeolite and toluene. This is supported by the fact that these sensors failed to fully return to baseline after each pulse of gas and it could mean that the gas fails to fully desorb from the sensing material. This effect was less pronounced at 450 °C. The sensors responded to 2.5 ppm of gas at all temperatures and when supplied with 10 ppm of the gas at 400 °C, the sensor coated with 3 layers of zeolite H-ZSM-5 gave a response ~5, providing a 1.8-fold increase in response over the unmodified $SnO_2$. When supplied with 50 ppm, the same sensor provided a 2.9-fold increase in response over the control. At 450 °C, its response was enhanced 3.8 times. These sensors did not reach steady state, probably due to the vapour's lagged diffusion into the sensitive layer. The sensors containing Na-A, however, responded very rapidly (<4 seconds in '1 layer Na-A' and '10 % (w/w) Na-A) and did reach steady state (Fig. 7). The enhancements obtained when compared to the control were, nevertheless, moderate i.e. 1.3-fold increase in the '1 layer Na-A' sensor. Sensors overlaid with H-Y zeolite were less responsive to toluene than the control, '1 layer of H-Y' showing a faster response than the sensor containing 3 layers of the zeolite, this could be directly related to the thickness of the zeolite film, delaying its access to the underlying $SnO_2$ material. It is possible that catalytic reactions at the sensor surface lead to reaction products to which $SnO_2$ was less responsive.

The admixed sensors were also very responsive to toluene, each sensor providing a distinctive response to the vapour. At 400 °C the response trends did not match that of the overlayers. Thus, H-ZSM-5 sensors were, once again, consistently sensitive to the vapour, 30 % (w/w) being more sensitive to toluene than its 10 % (w/w) counterpart at concentrations above 25 ppm. The sensor that contained 10 % (w/w) H-Y was consistently more sensitive than the 30 % (w/w) H-Y sensor. The latter failed to return to baseline following each gas pulse. Sensors containing Na-A zeolite were unresponsive at this temperature. At 450 °C Na-A sensors were sensitive to the gas, leading to very fast response times and they reached steady state. The remaining sensors continued to show shark-fin shapes.

When the Na-A zeolite sensors were exposed to toluene, their responses were very moderately improved when compared to the control. The sensor containing '1 layer of Na-A' improved by a factor of ~1.3 and the one with 3 layers by 1.1. The hydrophilicity of zeolite Na-A resulted in poor affinity to toluene and its large kinetic diameter prevented its straightforward access to the control

material. Having only 1 layer of zeolite produced a minor catalytic effect improving the sensitivity towards toluene, the response time of which was much faster than that obtained with a thicker filtering layer, as expected.

*Sensor Exposure to Carbon Monoxide.* Tests towards CO (kinetic diameter 3.76 Å) showed virtually no response to the gas from 50 to 250 ppm. When exposing both admixed and overlayered sensors to 400 ppm and 500 ppm the sensors began showing a response (refer to Figure S1 in ESI for an illustration of this). The admixed sensors provided fast responses to the gas, suggesting the full combustion of the CO vapour to $CO_2$ and $H_2O_{(v)}$. Sensors coated with zeolites were slightly more responsive to the gas than the admixed ones. It is possible that this is due to the fact that the direct interaction between the CO gas and the zeolite coating results in higher sensitivity to the gas than when it comes into contact to a surface that contains a mixture of the $SnO_2$ control and the zeolite. As can be seen in Figure S1 the relative response of the control sensor to CO is very low ($R_0/R$ = ~1.3). Once again it was interesting to see how differently the composition of the sensors affects gas response: while the sensors coated with zeolite Na-A responded to the gas, those admixed with the same zeolite did not.

Gosh et al (2014) provide a detailed account on the detection of CO with $SnO_2$ based sensors. Whilst other groups have detected lower concentrations of the gas at levels of, for instance, 30 ppm, achieving short recovery times (in the order of seconds) has previously been reported as an issue. The results presented here are promising as very fast response and recovery times were achieved. Nevertheless, further tests should be carried out to improve detection at lower concentrations.

*Sensor Exposure to Humid Air.* The sensors were exposed to humid air from 250 – 500 °C whilst increasing the supplied RH (%) from 5 – 50 % (Fig. 10). All overlaid and admixed sensors were responsive to humid air across the temperatures tested. As can be seen in Fig. 10, the peak shapes were particularly interesting ; they saturated very quickly and then presented an increase in sensor resistance for the duration of the humid-air pulse. Although the reason why the sensors appear to undergo multistep reactions is unclear, it is thought it could be an effect of the water vapour blocking any further adsorption of oxygen and thus a progressive decrease of electron transfer back to the $SnO_2$ could potentially lead to this behaviour. The initial decrease in resistance in the presence of water is This occurred at all the RHs tested. For the majority of the sensors there was a very minor increase in the response with higher RH, but this enhancement was more pronounced in the sensor containing 3 layers of Na-A, due to its hydrophilic nature. All the zeolite-containing sensors were more sensitive to water vapour than the control.

Admixed sensors also provided higher sensing responses to humid air than the control sensor, which had similar responsivity to water vapour at 400 °C and 450 °C. The admixed sensors that contained a higher zeolite loading were less responsive to water vapour than their counterparts. Once again there was a slight increase in sensitivity to water vapour as the RH (%) was increased. Water sensitivity was almost suppressed for the sensor with 30 % (w/w) H-Y between 250-350 °C. The sensor that showed higher affinity towards increased concentration of humid air (25 % RH) at 450 °C was that admixed with 10 % (w/w) H-ZSM-5.

In the SEM micrographs it was observed that zeolite Na-A was poorly visible in the mixtures and it is possible that the microstructure and smaller particle size of zeolite H-ZSM-5, when compared to Na-A, lead to more surface-reactive sites for water to interact and pass through the pores and inter-crystalline cavities, displacing the chemisorbed oxygen and leading to the specified decrease in resistance.(20) With the exception of the 30 % H-Y and 10 % H-ZSM-5 sensors, which gave distinct sensor responses, the rest behaved very similarly.

*Testing to Ethane in the Presence of Humid Air.* All the sensors tested behaved as n-type when they were exposed to a mixture of ethane with humid air. Exposing the overlaid sensors to a mixture of 50 ppm ethane and 10% RH, followed by a pulse of 50 ppm ethane with humid air corresponding to 25% RH illustrated the sensors' selectivity towards water vapour and suppression towards ethane (Fig. 11). It can be seen that the resistive behaviour first encountered upon exposure to just ethane in dry air was no longer visible and the sensors exhibited n-type behaviour, with peak shapes resembling that obtained with exposure to just humid air.

Although at 350 °C the overlaid sensors' responsivity to 50 ppm of ethane vapour was practically suppressed ($R/R_0 < 1.5$ as illustrated in Fig. 8), the resistance increased when supplied with the gas. In the humidity-ethane environment, however, water vapour molecules compete with ethane molecules, preventing ethane from accessing the sensitive layer. This led all sensors to respond conductively, showing an increase in conductivity when exposed to the target gas. Nevertheless, the interference brought about by ethane vapour caused the response to humid air to be partially reduced. This is in line with other studies in the literature that looked at water interference.(16, 20)

Similarly, when the admixed sensors were exposed to ethane in the presence of humid vapour at 350 °C, the response could mostly be attributed to water vapour as, once again, conductive responses were attained. The responses given by sensors '10 % and 30 % (w/w) Na-A', however, provided different peak shapes and the sensitivity was slightly enhanced, when compared to the results obtained with the supply of just water vapour. This could mean that a new reaction product was formed, to which 10 % (w/w) Na-A was particularly responsive ($R_0/R$ ~5.6) when mixed with 50 ppm ethane and 10 % RH. The response obtained with '10 % (w/w) H-ZSM-5' sensor, which was particularly sensitive to just water vapour (Fig. 10B) was also diminished when exposed to a mixture of ethane and humid air. It is possible that the pores of H-ZSM-5 saturate quicker in the presence of water and a larger molecule like ethane. When $SnO_2$ was admixed with zeolite H-Y, it could be seen that while the response towards just water vapour was essentially suppressed, the sensitivity was slightly enhanced with the introduction of ethane. Bearing in mind that as part of the combustion process of ethane water is produced, it is possible that this enhancement is a result of more water molecules being adsorbed into the pores of this zeolite, which may block the direct interaction of ethane with the zeolite.

## 4.0 Conclusions

It was found here that the modification of the control material by zeolite incorporation induced great improvements in the sensitive and selective capabilities of thick film $SnO_2$ based sensors. The microstructure obtained when fabricating admixtures seemed key to detect hydrocarbons and the responses were considerably better than those obtained with the overlayers. When exposing the sensors to straight chain alkanes it is possible that through reaction processes occurring in the sensing element, the target vapour converts to an oxidising molecule, consequently affecting the expected behaviour of an n-type material and turning it into p-type. This behaviour was more commonly seen in the admixed sensors.

The sensing arrays were successful in discriminating among gases that were very similar in structure. Discrimination was achieved as a result of the different frameworks and pore structures of the zeolites chosen, as well as through their different hydrophobic/hydrophilic characters. This enabled a better understanding of how the sensors can be strategically designed to respond to some molecules and less so to others. Furthermore, the arrays also displayed excellent features often sought in gas sensing such as selectivity, stability, rapid response and recovery times, exhibiting linearity at trace concentrations and capability of vapour trace detection of hazardous substances. It was revealed that temperature modulation of sensors might prove very useful in discriminating between molecules of similar kinetic diameter. The responses towards the straight-chain alkanes were significantly improved when compared to the control sensor.

Future work will involve feature selection analysis to understand the sensors and the features necessary to select an array fully capable of discriminating among gases.

## Acknowledgements

The authors acknowledge Dr Dewi Lewis for his expertise in zeolites, Martin Vickers and Dr Tom Gregory for their technical support. Financial support was provided by the EPSRC grant code EP/G037264/1 as part of UCL's Security Science Doctoral Training Centre.

## Notes and references

1. G. F. Fine, L. M. Cavanagh, A. Afonja, R. Binions, Metal oxide semi-conductor gas sensors in environmental monitoring. Sensors (Basel, Switzerland) 10, (2010) 5469.
2. D. E. Williams, Semiconducting oxides as gas-sensitive resistors. Sensors and Actuators B: Chemical 57, (1999) 1.
3. K. Wetchakun, T. Samerjai, N. Tamaekong, C. Liewhiran, C. Siriwong, V. Kruefu, A. Wisitsoraat, A. Tuantranont, S. Phanichphant, Semiconducting metal oxides as sensors for environmentally hazardous gases. Sensors and Actuators B: Chemical 160, (2011) 580.
4. M. Bart, D. E. Williams, B. Ainslie, I. McKendry, J. Salmond, S. K. Grange, M. Alavi-Shoshtari, D. Steyn, G. Henshaw, High Density Ozone Monitoring Using Gas Sensitive Semi-Conductor Sensors in the Lower Fraser Valley, British Columbia. Environmental Science & Technology 48, (2014/04/01, 2014) 3970.
5. L. Spinelle, M. Gerboles, M. G. Villani, M. Aleixandre, F. Bonavitacola, Field calibration of a cluster of low-cost available sensors for air quality monitoring. Part A: Ozone and nitrogen dioxide. Sensors and Actuators B: Chemical 215, (2015) 249.
6. W. J. Peveler, R. Binions, S. M. V. Hailes, I. P. Parkin, Detection of explosive markers using zeolite modified gas sensors. Journal of Materials Chemistry A 1, (2013) 2613.
7. Z. Haddi, A. Amari, N. E. Bari, E. Llobet, B. Bouchikhi, A portable electronic nose system for the identification of cannabis-based drugs. Sensors and Actuators B: Chemical 155, (2011) 456.
8. P. T. Hernández, A. J. T. Naik, E. J. Newton, S. M. V. Hailes, I. P. Parkin, Assessing the potential of metal oxide semiconducting gas sensors for illicit drug detection markers. J Mater Chem A 2, (2014) 8952.
9. S. Moltchanov, I. Levy, Y. Etzion, U. Lerner, D.M. Broday, B. Fishbain, On the feasibility of measuring urban air pollution by wireless distributed sensor networks. The Science of the total environment 502, (2015) 537.
10. S.-W. Chiu, K.-T. Tang, Towards a chemiresistive sensor-integrated electronic nose: a review. (2013), vol. 13, pp. 14214-47.
11. N. Yamazoe, K. Shimanoe, Proposal of contact potential promoted oxide semiconductor gas sensor. Sensors and Actuators B: Chemical 187, (2013) 162.
12. G. Korotcenkov, The role of morphology and crystallographic structure of metal oxides in response of conductometric-type gas sensors. Materials Science and Engineering: R: Reports 61, (2008) 1.
13. G. Korotcenkov, B. K. Cho, Engineering approaches for the improvement of conductometric gas sensor parameters. Sensors and Actuators B: Chemical 188, (2013) 709.
14. R. Binions, A. Afonja, S. Dungey, D.W. Lewis, I.P.Parkin, D.E. Williams, Discrimination effects in zeolite modified metal oxide semiconductor gas sensors. IEEE Sensors Journal 11, (2011) 1145.
15. M. Fleischer, H. Meixner, Selectivity in high-temperature operated semiconductor gas-sensors. Sensors and Actuators B: Chemical 52, (1998) 179.
16. M. Vilaseca, J. Coronas, A. Cirera, A. Cornet, J.R. Morante, J. Santamaria, Development and application of micromachined Pd/$SnO_2$ gas sensors with zeolite coatings. Sensors and Actuators B: Chemical 133, (2008) 435.

17. P. Varsani, A. Afonja, D. E. Williams, I. P. Parkin, R. Binions, Zeolite-modified $WO_3$ gas sensors - Enhanced detection of NO2. Sensors and Actuators B: Chemical 160, (2011) 475.
18. A. Afonja, R. Binions, S. Dungey, I.P.Parkin, D. W. Lewis, D. E. Williams, Zeolites as transformation elements in discriminating semiconductor metal oxide sensors. Procedia Engineering 5, (2010) 103.
19. K. Sahner, R. Moos, M. Matam, J. J. Tunney, M. Post, Hydrocarbon sensing with thick and thin film p-type conducting perovskite materials. Sensors and Actuators B: Chemical 108, (2005) 102.
20. M. Vilaseca, J. Coronas, A. Cirera, A. Cornet, J. R. Morante, J. Santamaria, Use of zeolite films to improve the selectivity of reactive gas sensors. Catalysis Today 82, (2003) 179.
21. S. R. Morrison, Selectivity in semiconductor gas sensors. Sensors and Actuators 12, (1987) 425.
22. M. Vilaseca, J. Coronas, A. Cirera, A. Cornet, J. R. Morante, J. Santamaria, Gas detection with $SnO_2$ sensors modified by zeolite films. Sensors and Actuators B: Chemical 124, (2007) 99.
23. S. Reiß, G. Hagen, R. Moos, Zeolite-based Impedimetric Gas Sensor Device in Low-cost Technology for Hydrocarbon Gas Detection. Sensors 8, (2008) 7904.
24. K. Sahner, G. Hagen, D. Schönauer, S. Reib, R. Moos, Zeolites - versatile materials for gas sensors. Solid State Ionics 179, (2008) 2416.
25. D. P. Mann, K. F. E. Pratt, T. Paraskeva, I. P. Parkin, D. E. Williams, Transition Metal Exchanged Zeolite Layers for Selectivity Enhancement of Metal-Oxide Semiconductor Gas Sensors. IEEE Sensors Journal 7, (2007) 551.
26. Y. Zheng, Z. Li, P. K. Dutta, Exploitation of unique properties of zeolites in the development of gas sensors. Sensors 12, (2012) 5170.
27. D. C. Pugh, E. J. Newton, A. J. T. Naik, S. M. V. Hailes, I. P. Parkin, The gas sensing properties of zeolite modified zinc oxide. J Mater Chem A 2, (2014) 4758.
28. G. Hagen, A. Dubbe, G. Fischerauer, R. Moos, Thick-film impedance based hydrocarbon detection based on chromium(III) oxide/zeolite interfaces. Sensors and Actuators B: Chemical 118, (2006) 73.
29. J. Coronas, J. Santamaria, The use of zeolite films in small-scale and micro-scale applications. Chemical Engineering Science 59, (2004) 4879.
30. O. Hugon, M. Sauvan, P. Benech, C. Pijolat, F. Lefebvre, Gas separation with a zeolite filter, application to the selectivity enhancement of chemical sensors. Sensors and Actuators B: Chemical 67, (2000) 235.
31. G. Hagen, A. Dubbe, F. Rettig, A. Jerger, Th. Birkhofer, R. Müller, C. Plog, R. Moos, Selective impedance based gas sensors for hydrocarbons using ZSM-5 zeolite films with chromium(III)oxide interface. Sensors and Actuators B: Chemical 119, (2006) 441.
32. K. Sahner, G. Hagen, D. Schonauer, S. Reis, R. Moos, Zeolites — Versatile materials for gas sensors. Solid State Ionics 179, (2008) 2416.
33. D. C. Pugh, S. M. V. Hailes, I. P. Parkin, A gas-sensing array produced from screen-printed zeolite-modified chromium titanate. Measurement Science and Technology 26, (2015) 1.
34. G. Korotcenkov, Metal oxides for solid-state gas sensors: What determines our choice? Materials Science and Engineering B 139, (2007) 1.
35. P. M. Sousa, A. J. Silvestre, N. popovici, O. Conde, Morphological and structural characterization of $CrO_2/Cr_2O_3$ films grown by laser-CVD. Applied Surface Science 247, (2005) 423.
36. D. E. Williams, Semiconducting oxides as gas-sensitive resistors. Sensors and Actuators B: Chemical 57, (1999) 1.
37. H. Meixner, U. Lampe, Metal Oxide Sensors. Sensors and Actuators B 33, (1996) 198.
38. K. Sahner, M. Fleischer, E. Magori, H. Meixner, J. Deerberg, R. Moos, HC-sensor for exhaust gases based on semiconducting doped $SrTiO_3$ for On-Board Diagnosis. Sensors and Actuators B: Chemical 114, (2006) 861.
39. S. D. Bakrania, M. S. Wooldridge, The effects of two thick film deposition methods on tin dioxide gas sensor performance. Sensors 9, (2009) 6853.

40. C. Song, J. M. Garcés, Y. Sugi, Chapter 1 Introduction to Shape-Selective Catalysis. ACS Symposium Series, American Chemical Society: Washington DC, (1999) 1.
41. K. Yin, F. Liao, Y Zhu, A. Gao, T. Wang, M. Shao, Enhanced gas-sensing response by gamma ray irradiation: $Ag/Ag_2SnO_3$ nanoparticle-based sensor to ethanol, nitromethane and acetic acid.
42. B. Freeman, Y. Yampolskii, I. Pinnau, Materials Science of Membranes for Gas and Vapour Separation. (John Wiley & Sons, West Sussex, England, 2006)

## Figure Captions

Caption 1: Schematic of the sensor fabrication procedure, highlighting the differences between the control sensor and ones containing overlayers or admixtures. A sensor with spot-welded platinum wires and a sensor bonded onto the polyphenylene sulphide housing have also been included.

Caption 2: XRD patterns of $SnO_2$ overlaid and admixed with zeolite H-ZSM-5. $SnO_2$ has been indexed in accordance with references found in the literature.(35) Note that indexed peaks correspond only to the control material.

Caption 3: SEM micrographs of the admixed sensors taken at a magnification of x10000. (A) $SnO_2$ with 10 % (w/w) H-Y. (B) $SnO_2$ with 10 % (w/w) H-ZSM-5. (C) $SnO_2$ with 10 % Na-A. (D) $SnO_2$ with 30 % (w/w) H-Y. (E) $SnO_2$ with 30% (w/w) H-ZSM-5. (F) $SnO_2$ with 30 % (w/w) Na-A

Caption 4: Cross-section of $SnO_2$ sensor chip coated with 3 layers of zeolite H-ZSM-5 taken on a Hitachi S-3400N microscope operated at 5 kV using a working distance of 16.3 mm.

Caption 5: Control $SnO_2$ sensor exposure to 100 ppm of ethane, propane, butane, ethanol, isopropanol, 10 ppm acetone and 50 ppm toluene across temperatures ranging between 250- 500 °C.

Caption 6: Sensor responses at 450 °C when supplied with the maximum concentration of test gas according to zeolite group and fabrication method. (A) Overlaid sensor responses and (B) Admixed sensor responses. The kinetic diameters (Å) of the molecules used have been included in brackets.

Caption 7: Sensor responses to the maximum supplied concentrations at 450 °C together with the response times, $t_{90}$. Additional information regarding the zeolite pore diameters and the kinetic diameters of the molecules tested have also been included.

Caption 8: (A) Admixed resistive sensor responses to ethane when exposed to 10 ppm, 20 ppm, 50 ppm, 80 ppm and 100 ppm. (B) Admixed resistive sensor responses to butane vapour when exposed to concentrations ranging between 10 - 100 ppm. (C) Overlaid resistive sensor responses to ethane vapour concentrations ranging between 5 ppm, 10 ppm, 20 ppm, 50 ppm, 80 ppm and – 100 ppm. (D) Overlaid conductive sensor responses to butane vapour at concentrations ranging between 5 – 100 ppm. Tests were performed at 350 °C.

Caption 9: Overlaid sensor responses to increased concentrations (ppm) of IPA, ethanol, toluene and acetone vapours at 450 °C.

Caption 10: (A) Overlaid sensor exposure to humid air corresponding to 5% - 50% RH. (B) Admixed sensor exposure to humid air corresponding to 5% - 50% RH. All tests were performed at 350 °C.

Caption 11: (A) Overlaid sensor exposure to 50 ppm ethane in 10% RH (first gas pulse) and 25% RH (second gas pulse). (B) Admixed sensor exposure to 50 ppm ethane in 10% RH (first gas pulse) and 25%RH (second gas pulse). All tests were performed at 350 °C.

S1 ESI: Sensor responses to different concentrations of carbon monoxide vapour at 450 °C. The top figure illustrates the admixed sensor responses to the gas and the bottom figure that of the overlayered sensor responses.

## Figures Sensors & Actuators $SnO_2$ paper

### Figure 1

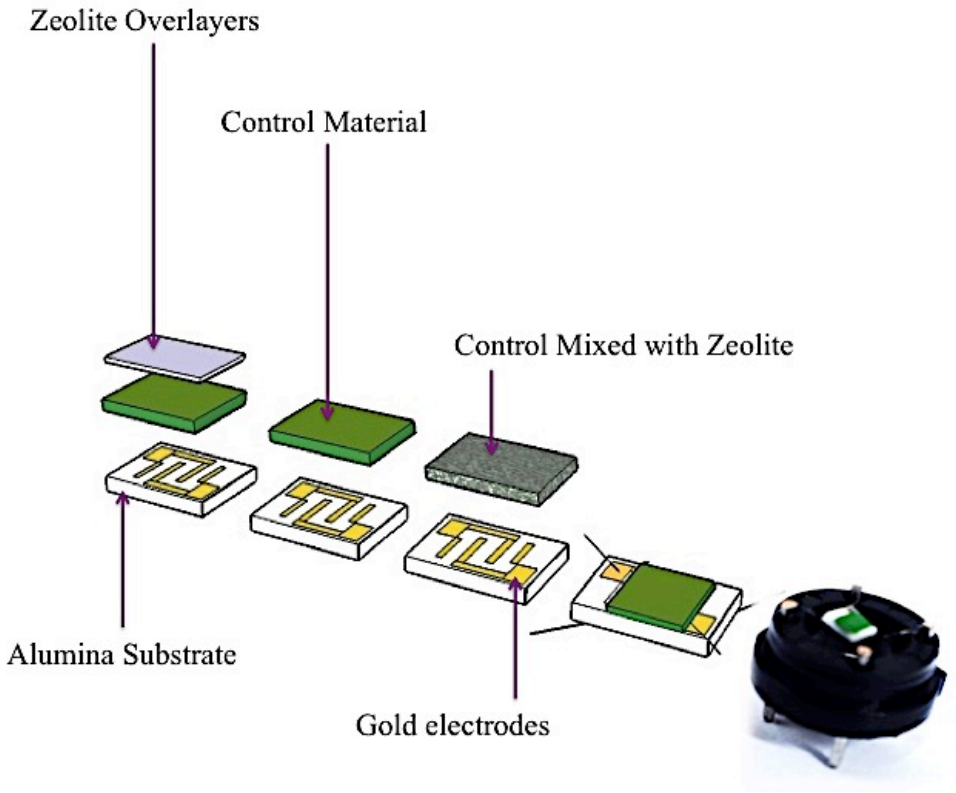
Zeolite Overlayers
Control Material
Control Mixed with Zeolite
Alumina Substrate
Gold electrodes

Fig 2

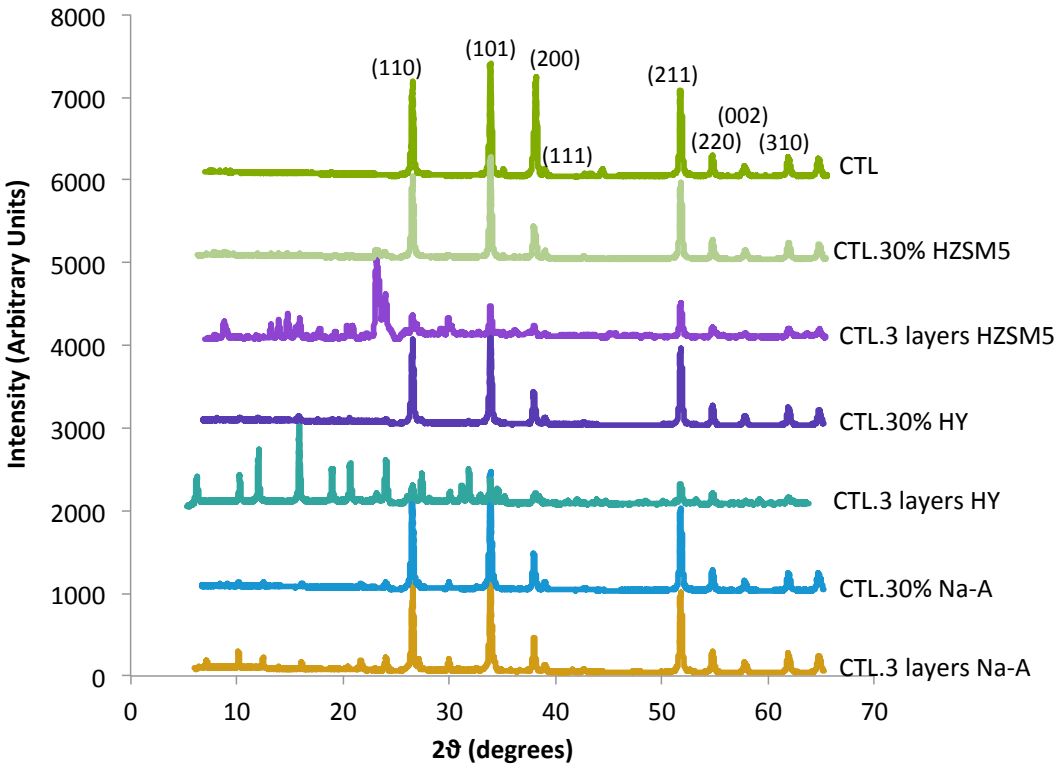
8000
7000
6000
5000
4000
3000
2000
1000
0
Intensity (Arbitrary Units)
0
10
20
30
40
50
60
70
2ϑ (degrees)
(110)
(101)
(200)
(111)
(211)
(002)
(220)
(310)
CTL
CTL.30% HZSM5
CTL.3 layers HZSM5
CTL.30% HY
CTL.3 layers HY
CTL.30% Na-A
CTL.3 layers Na-A

Figure 3

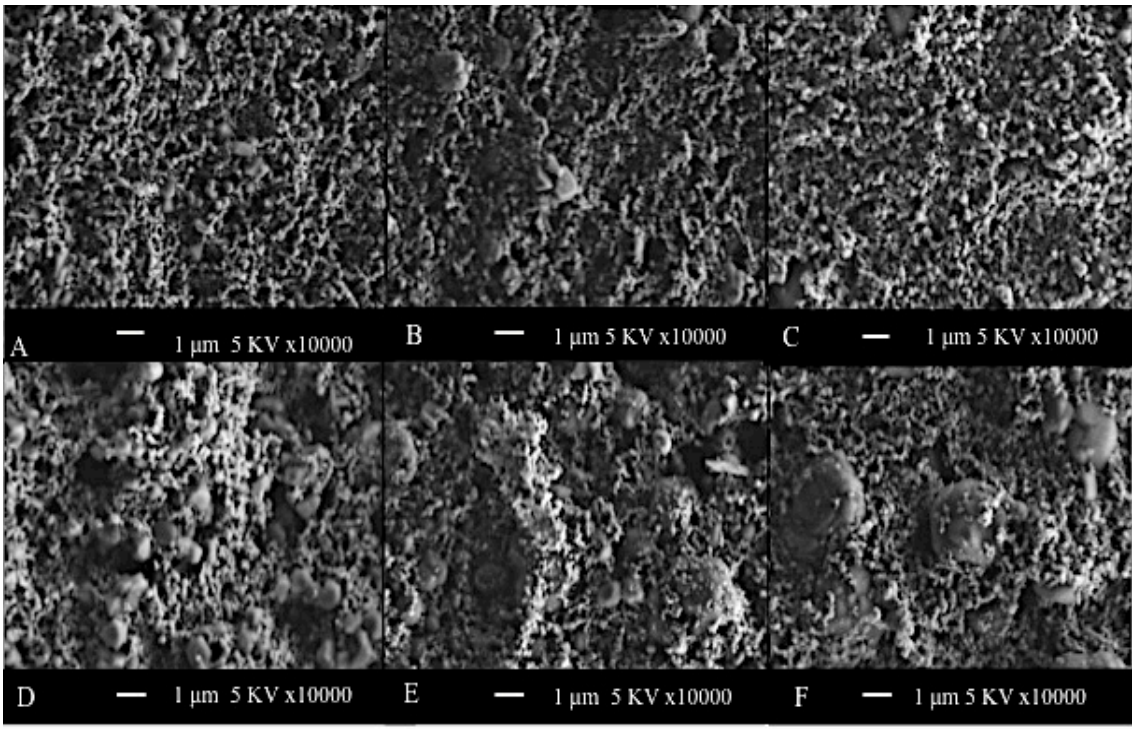


Figure 4

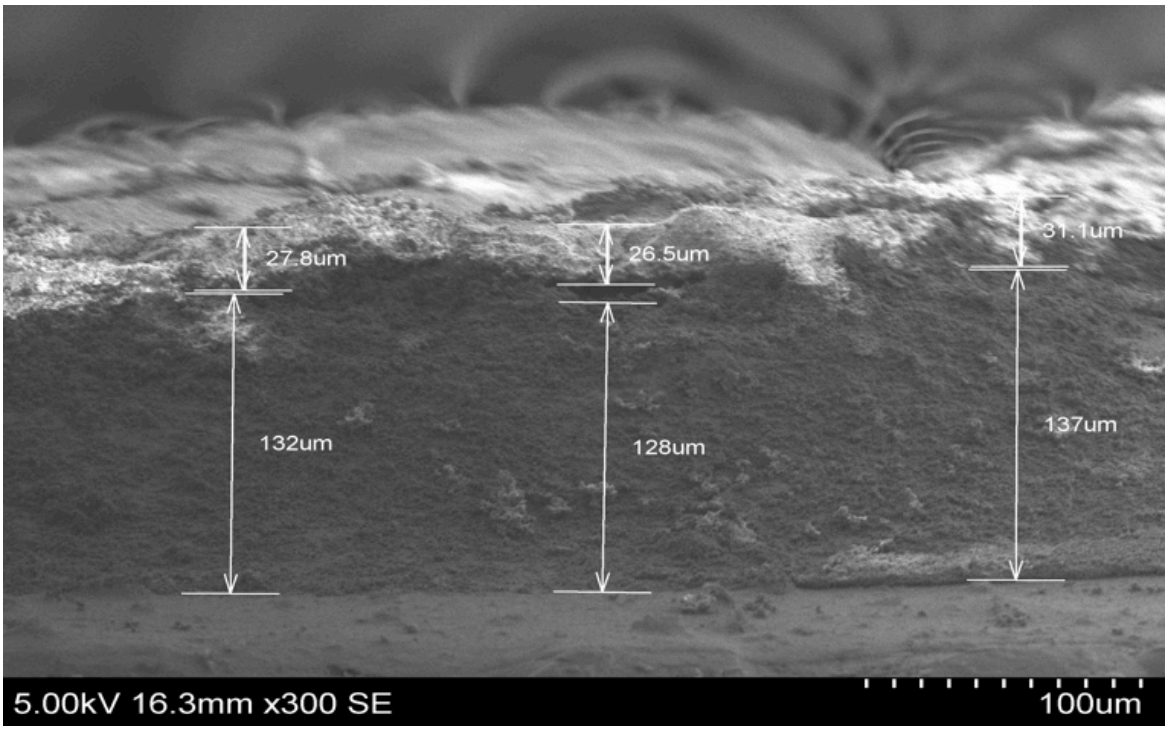

Figure 5

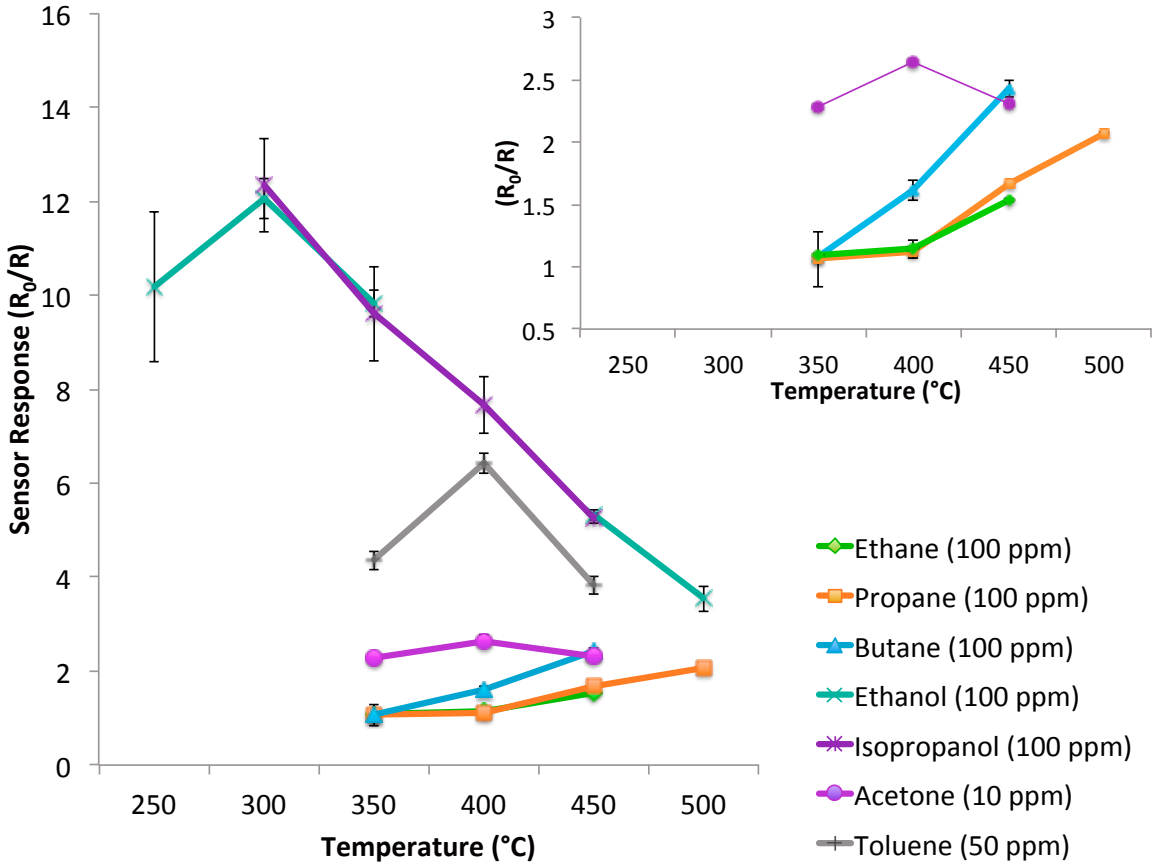
16
14
12
10
8
6
4
2
0
Sensor Response ($R_0/R$)
250
300
350
400
450
500
Temperature (°C)
3
2.5
2
1.5
1
0.5
($R_0/R$)
250
300
350
400
450
500
Temperature (°C)
Ethane (100 ppm)
Propane (100 ppm)
Butane (100 ppm)
Ethanol (100 ppm)
Isopropanol (100 ppm)
Acetone (10 ppm)
Toluene (50 ppm)

Figure 6

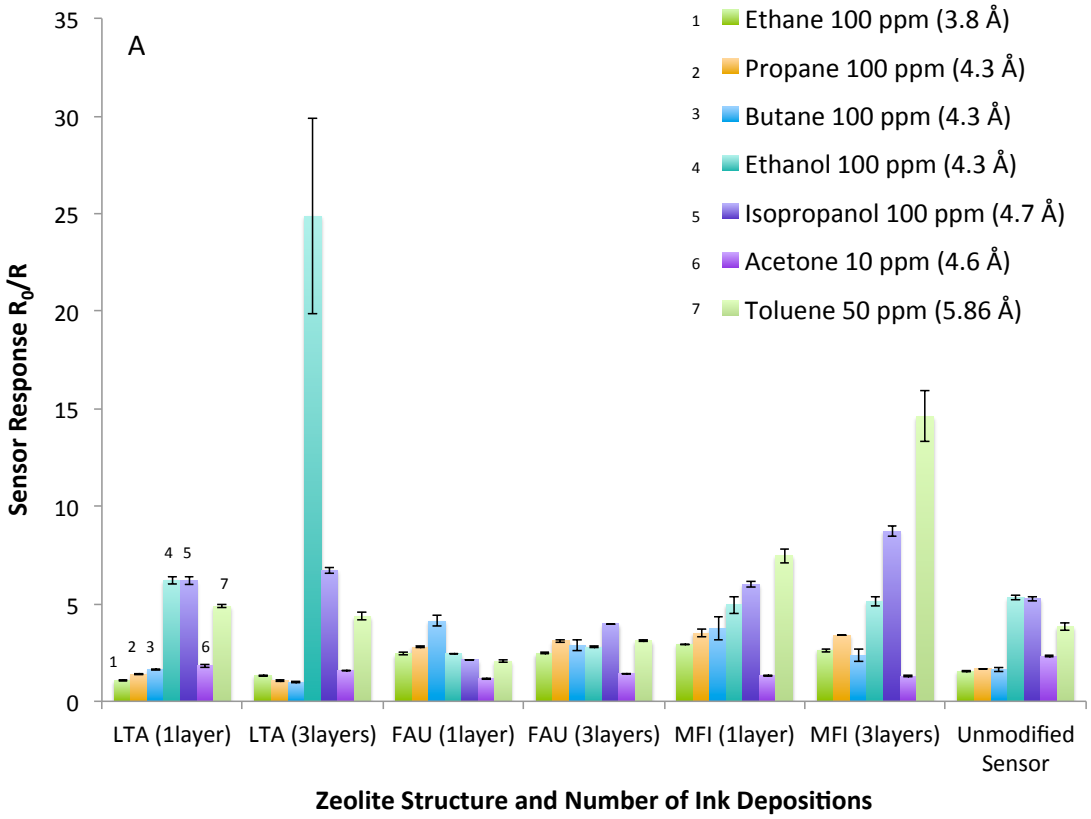
A
1 Ethane 100 ppm (3.8 Å)
2 Propane 100 ppm (4.3 Å)
3 Butane 100 ppm (4.3 Å)
4 Ethanol 100 ppm (4.3 Å)
5 Isopropanol 100 ppm (4.7 Å)
6 Acetone 10 ppm (4.6 Å)
7 Toluene 50 ppm (5.86 Å)
Sensor Response $R_0/R$
0
5
10
15
20
25
30
35
LTA (1layer)
LTA (3layers)
FAU (1layer)
FAU (3layers)
MFI (1layer)
MFI (3layers)
Unmodified Sensor
Zeolite Structure and Number of Ink Depositions

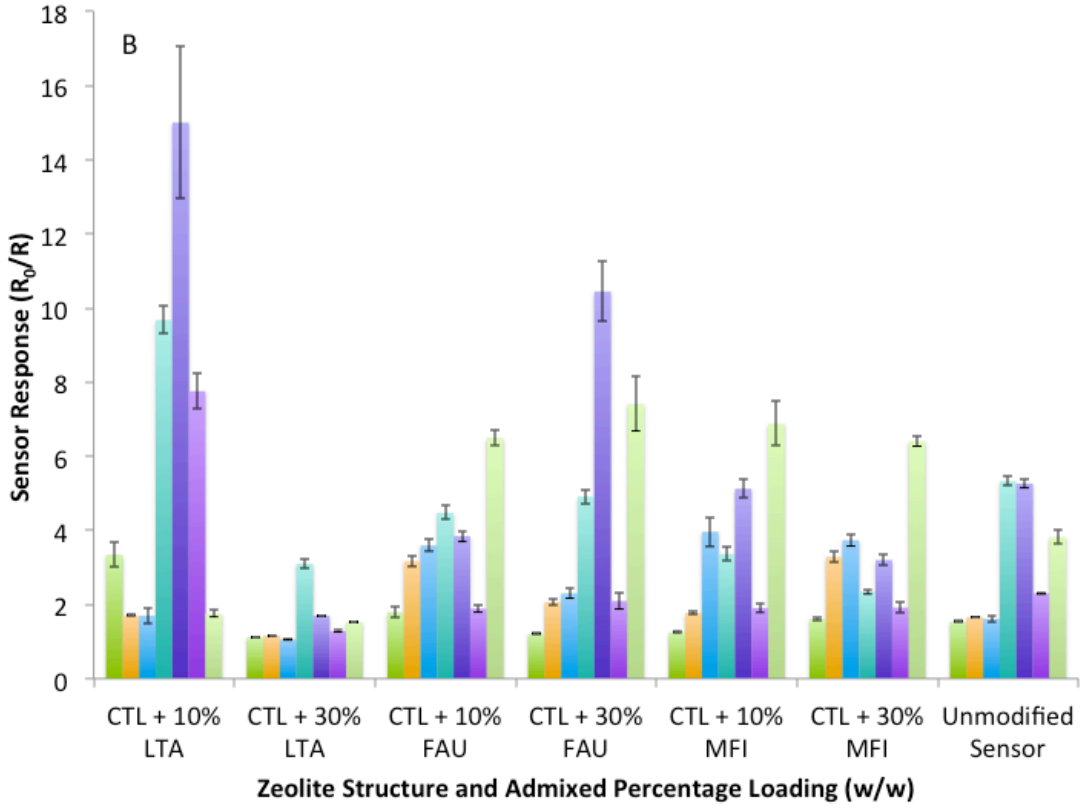
B
Sensor Response ($R_0/R$)
0
2
4
6
8
10
12
14
16
18
CTL + 10% LTA
CTL + 30% LTA
CTL + 10% FAU
CTL + 30% FAU
CTL + 10% MFI
CTL + 30% MFI
Unmodified Sensor
Zeolite Structure and Admixed Percentage Loading (w/w)

Figure 7

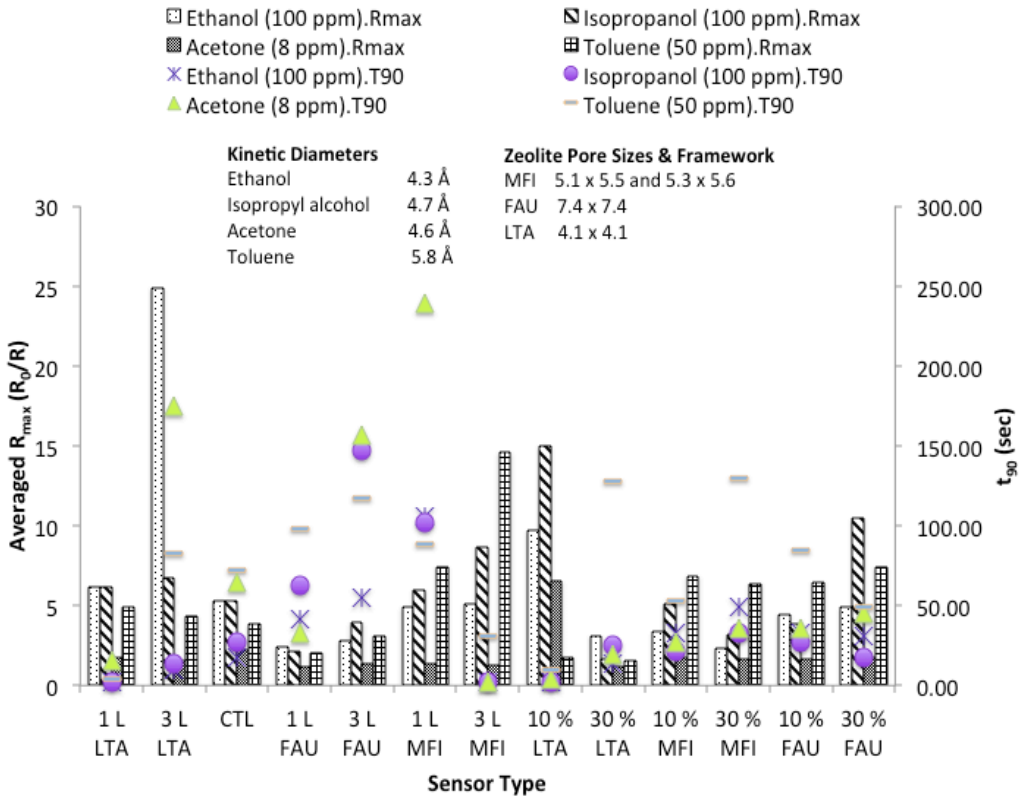


Figure 8

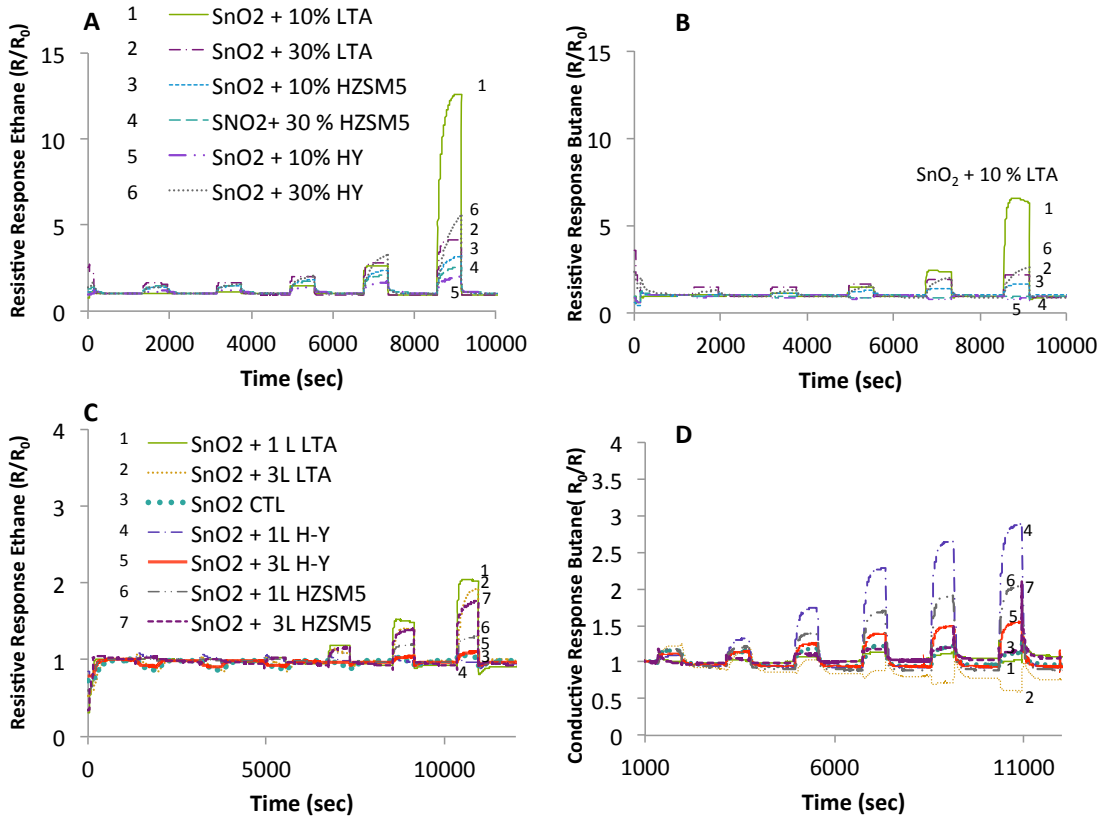

Figure 9

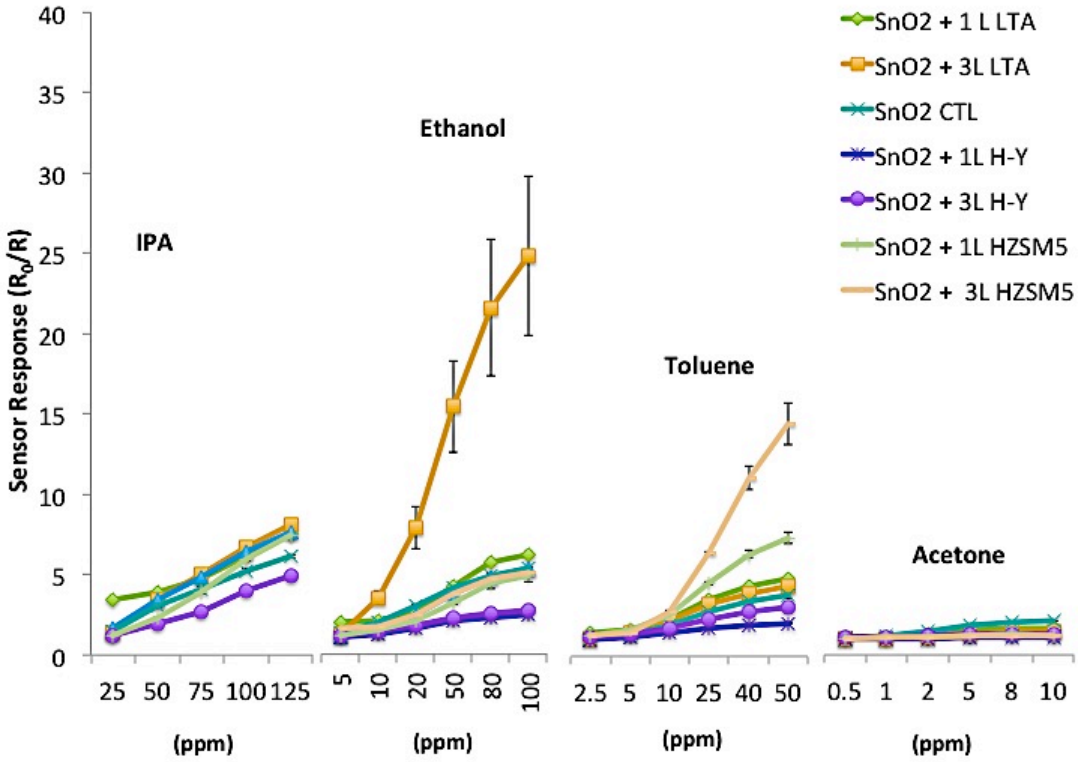
Sensor Response ($R_0$/R)
40
35
30
25
20
15
10
5
0
IPA
Ethanol
Toluene
Acetone
25 50 75 100 125
5 10 20 50 80 100
2.5 5 10 25 40 50
0.5 1 2 5 8 10
(ppm)
(ppm)
(ppm)
(ppm)
SnO2 + 1 L LTA
SnO2 + 3L LTA
SnO2 CTL
SnO2 + 1L H-Y
SnO2 + 3L H-Y
SnO2 + 1L HZSM5
SnO2 + 3L HZSM5

Figure 10

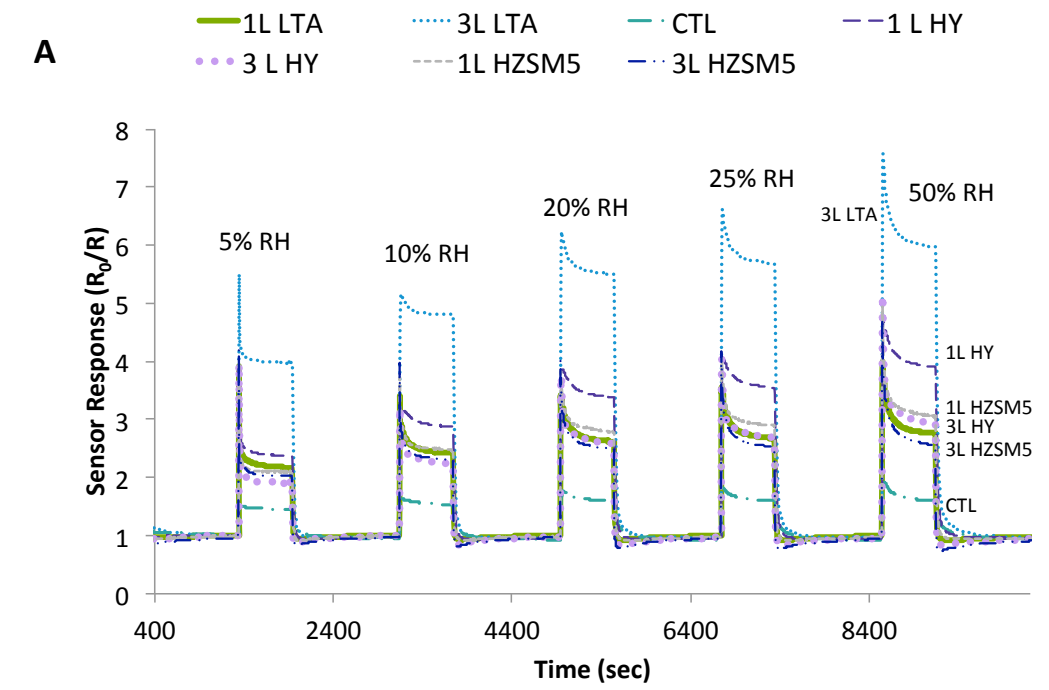
A
1L LTA
3L LTA
CTL
1 L HY
3 L HY
1L HZSM5
3L HZSM5
Sensor Response (R0/R)
Time (sec)
5% RH
10% RH
20% RH
25% RH
50% RH
3L LTA
1L HY
1L HZSM5
3L HY
3L HZSM5
CTL

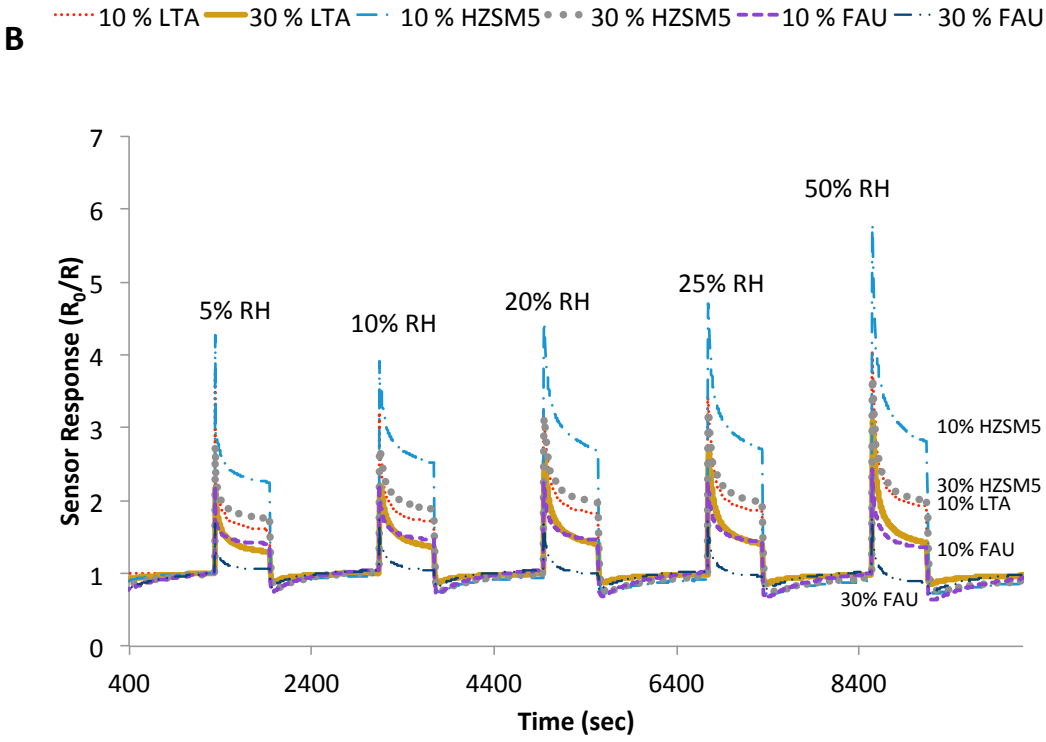
B
10 % LTA
30 % LTA
10 % HZSM5
30 % HZSM5
10 % FAU
30 % FAU
Sensor Response (R0/R)
Time (sec)
5% RH
10% RH
20% RH
25% RH
50% RH
10% HZSM5
30% HZSM5
10% LTA
10% FAU
30% FAU

Figure 11

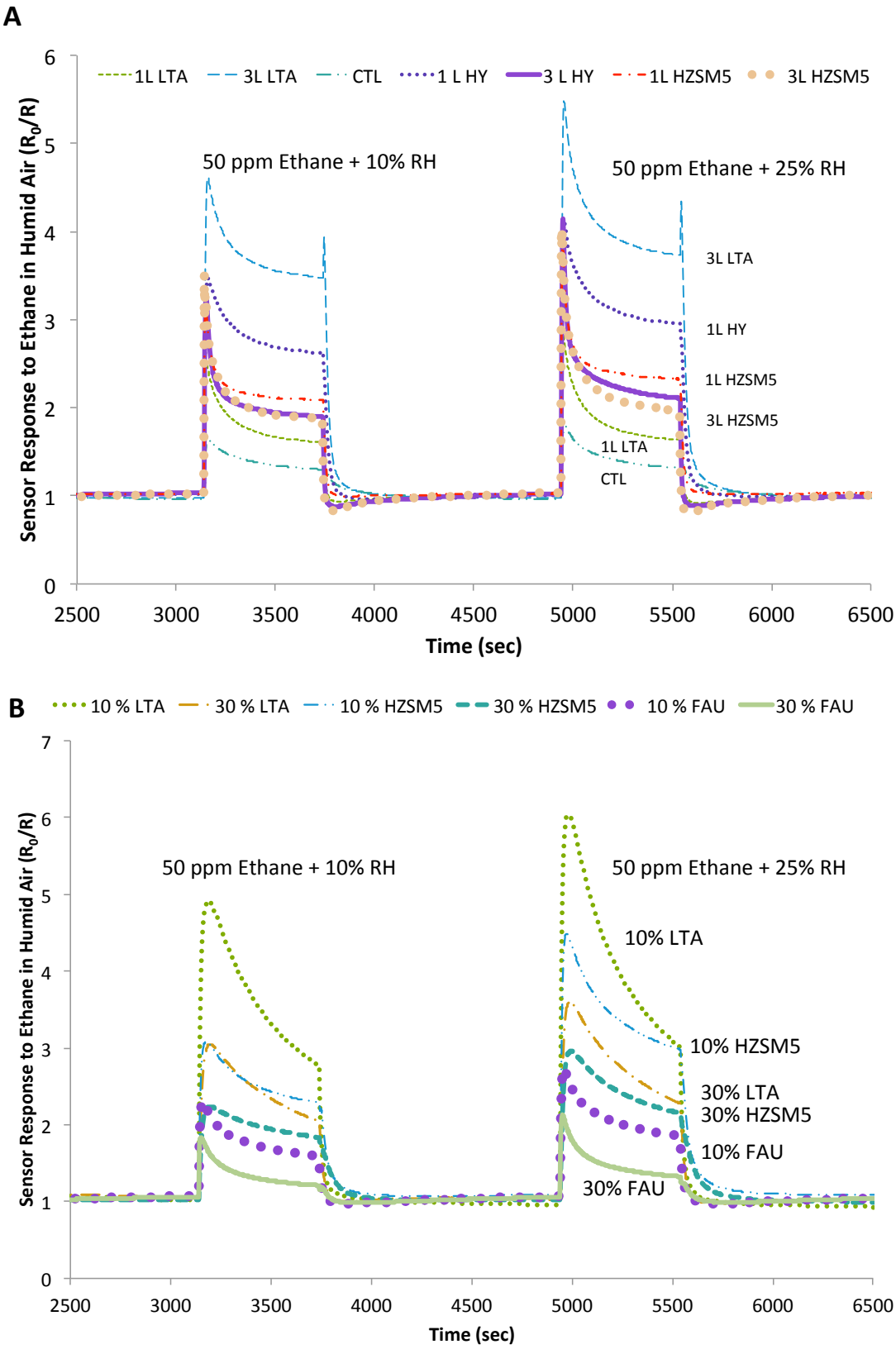
A
1L LTA
3L LTA
CTL
1 L HY
3 L HY
1L HZSM5
3L HZSM5
50 ppm Ethane + 10% RH
50 ppm Ethane + 25% RH
3L LTA
1L HY
1L HZSM5
3L HZSM5
1L LTA
CTL
Sensor Response to Ethane in Humid Air (R0/R)
Time (sec)
B
10 % LTA
30 % LTA
10 % HZSM5
30 % HZSM5
10 % FAU
30 % FAU
50 ppm Ethane + 10% RH
50 ppm Ethane + 25% RH
10% LTA
10% HZSM5
30% LTA
30% HZSM5
10% FAU
30% FAU
Sensor Response to Ethane in Humid Air (R0/R)
Time (sec)

TABLE 1

| | | Admixtures | | Overlayers | |
|---|---|---|---|---|---|
| Control Sensor | Zeolite Type | Zeolite percentage weight (%) | Admixture Sensor Names | Zeolite Coatings | Overlayer Sensor Names |
| $SnO_2$ (CTL) | H-ZSM-5 (MFI) | 10 | $SnO_2$ + 10% HZSM5 | 1 | $SnO_2$ + 1 L HZSM5 |
| | | 30 | $SnO_2$ + 30 % HZSM5 | 3 | $SnO_2$ + 3L HZSM5 |
| | Na-A (LTA) | 10 | $SnO_2$ + 10% LTA | 1 | $SnO_2$ + 1 L LTA |
| | | 30 | $SnO_2$ + 30 % HZSM5 | 3 | $SnO_2$ + 3 L LTA |
| | H-Y (FAU) | 10 | $SnO_2$ + 10% HY | 1 | $SnO_2$ + 1 L HY |
| | | 30 | $SnO_2$ + 30% HY | 3 | $SnO_2$ + 3 L HY |

ESI

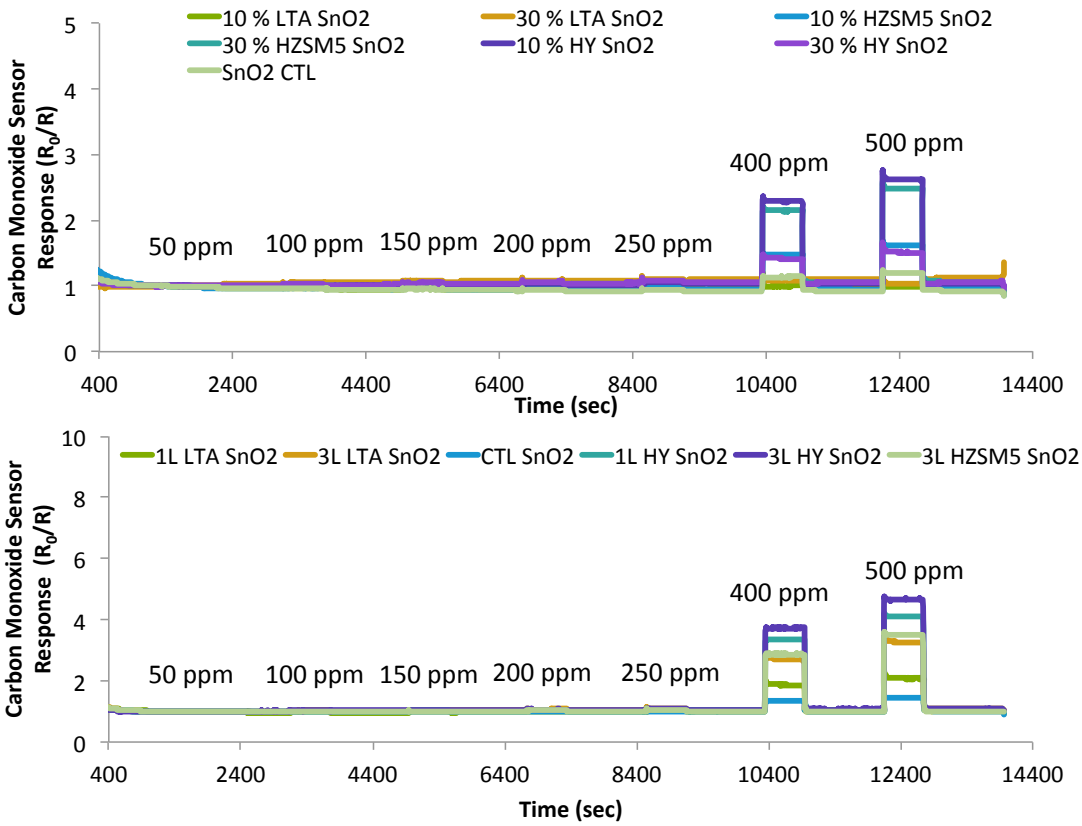
10 % LTA SnO2
30 % LTA SnO2
10 % HZSM5 SnO2
30 % HZSM5 SnO2
10 % HY SnO2
30 % HY SnO2
SnO2 CTL
Carbon Monoxide Sensor Response (R0/R)
50 ppm
100 ppm
150 ppm
200 ppm
250 ppm
400 ppm
500 ppm
Time (sec)
1L LTA SnO2
3L LTA SnO2
CTL SnO2
1L HY SnO2
3L HY SnO2
3L HZSM5 SnO2
Carbon Monoxide Sensor Response (R0/R)
50 ppm
100 ppm
150 ppm
200 ppm
250 ppm
400 ppm
500 ppm
Time (sec)